UNIVERSIDADE DE LISBOA
FACULDADE DE CIÊNCIAS
DEPARTAMENTO DE BIOLOGIA ANIMAL

Evaluation of sCD40L in heart regeneration after cryoinjury-induced myocardial infarction in Zebrafish – methodological approach

Patrícia Raquel dos Anjos Eugénio

Mestrado em Biologia Humana e Ambiente

Dissertação orientada por:
Doutora Patrícia Napoleão
Professora Ana Maria Viegas-Crespo

2016

AGRADECIMENTOS

Após um ano há a evidente necessidade de reconhecer como parte fundamental para concretizar o trabalho aqui exposto, uma lista que com o tempo foi crescendo. Contemos e somemos juntos a quantidade de "agradeço" (s), "agradecer" (es) e "obrigada" (s) a quem me acompanhou.

Como nunca poderia deixar de ser, agradeço, antes de mais à Doutora Patrícia Napoleão, com quem aprendi imenso, por me orientar nesta jornada, por estar sempre disponível para me ajudar com qualquer problema, ter uma enorme paciência para esclarecer todas as dúvidas (que não foram poucas, de todo) e capacidade de contornar obstáculos, mesmo quando o tempo mais apertava e o cansaço pesava. Esta tese não teria sido possível sem todo esse contributo.

À Professora Ana Viegas-Crespo, por ter aceite ser minha orientadora e disponibilizado o seu imenso conhecimento para revisão deste trabalho, como a excelente profissional que é.

Quero também deixar um obrigada à Professora Deodália Dias, coordenadora do Mestrado em Biologia Humana e Ambiente por me guiar, pacientemente, apoiar e também esclarecer qualquer dúvida que tivesse.

Não posso, de qualquer modo, deixar de agradecer também a todos os que no iMM me ajudaram, pertencentes ao grupo de trabalho e às *Facilities* indispensáveis no projecto. Assim, obrigado à Professora Carlota Saldanha por me ter recebido no seu laboratório e por ter proporcionado esta oportunidade. Obrigada à Teresa Freitas, sempre muito querida e disposta a ajudar. Ao Doutor Ângelo Calado que mais do que uma vez, me esclareceu dúvidas. À Lara e à Aida, à Aida e à Lara, a ambas, pelo companheirismo e simpatia com que me receberam na *Fish Facility*, sempre tranquilas e disponíveis para ajudar na resolução de qualquer problema que surgisse. Também ao António, que comigo percorreu quase tudo o

que era lupa e microscópio no iMM, me auxiliou e formou no *Light Sheet*, mesmo quando se encontrava com imenso trabalho para fazer.

E porque *parenthood* não vem com instruções, agradeço aos meus pais por todos os sacrifícios que fizeram por mim, naquela forma meio "cliché" que todo o mundo faz, mas que não deixa de ser verdadeira. Neste mesmo parágrafo agradeço às *friends*, poucas, mas boas, como se costuma dizer e melhor também não poderia pedir. O namorado também leva o seu "obrigada", por estar sempre comigo e ter acompanhado todo o trabalho que fiz este ano com interesse e entusiasmo. Obrigada por tudo.

Faço questão de agradecer às minhas gatas, por peculiar que pareça, *just bare with me*, Mafalda e Lady, mesmo não tendo forma de entender o que escrevo, quero deixar aqui salientado o valor que têm para mim, sempre.

Acima de tudo, esta é a parte que sempre soube como iria escrever. Assim, deixo para último a quem dedico tudo o que fiz no meu mestrado, desde o início, não tirando qualquer valor a quem já mencionei. Aos meus benfiquistas preferidos, o meu tio e o meu avô. A este ponto apenas posso imaginar a alegria e orgulho que vos daria verem o quão longe cheguei. Agradeço-vos por terem feito e fazerem parte da minha vida, permanentemente no meu coração a cada passo que dou. Esta tese é para vocês.

RESUMO

O enfarte agudo do miocárdio, ou ataque cardíaco, constitui uma das maiores causas de mortalidade e morbilidade no ser humano. De um modo geral, o enfarte tem como origem uma obstrução das artérias coronárias, em consequência da qual o tecido a jusante fica em isquemia, havendo necrose do mesmo. Como o coração humano é incapaz de regeneração, o miocárdio afectado cicatriza, num processo que envolve inflamação e reparação, o que origina a perda de contractilidade do miocárdio, podendo levar a insuficiência cardíaca.

O peixe-zebra (*Danio rerio*) não possui a limitação do potencial regenerativo, referida anteriormente, tendo já sido evidenciada a capacidade regenerativa de até 25% do ventrículo criocauterizado. Este organismo é um modelo adequado para estudos de desenvolvimento cardíaco e doenças humanas relacionadas, já que detém uma homologia com o ser humano na programação da expressão génica essencial, bem como na actividade eléctrica do coração.

Estudos anteriores do grupo de investigação onde esta tese foi realizada mostram níveis do ligando solúvel de CD40 (sCD40L), uma glicoproteína transmembranar, em pacientes de enfarte agudo do miocárdio está associado a disfunção endotelial persistente e a reparação cardíaca pós-enfarte comprometida. A associação da sCD40L à reparação e remodelação do miocárdio pós-enfarte não foi ainda explorada, pelo que é um tópico que carece de esclarecimentos. Para tal, estudos usando o modelo de peixe-zebra são necessários de forma a compreender os mecanismos associados ao papel de sCD40L na recuperação cardíaca após o enfarte do miocárdio.

Assim, o objectivo principal deste projecto foi a implementação de protocolos que permitiram avaliar o papel do sCD40L na regeneração do miocárdio

de peixe-zebra após enfarte agudo do miocárdio induzido por uma sonda a frio. Para atingir o objectivo, foram estabelecidos vários protocolos como a criolesão, a colheita de sangue, metodologias histológicas e de microscopia. O projecto também visou a implementação do protocolo de um Modelo de Regeneração Comprometida, contribuindo para o objectivo principal proposto.

Prospectivamente, esta dissertação pode contribuir para estudos futuros em peixe-zebra, que porventura providenciarão translação para investigação clínica envolvendo reparação cardíaca pós-enfarte, em pacientes humanos.

Para cumprir o objectivo proposto, os peixes-zebra adultos, foram sujeitos a criolesão de modo a induzir um enfarte do miocárdio e, por conseguinte, monitorizados em vários pontos temporais. Um modelo de regeneração comprometida foi também estudado, através da administração de glucocorticóides imunossupressores aos peixes. A sCD40L foi avaliada no sangue recorrendo a *Enzyme-Linked Immunosorbent Assay* (ELISA). Técnicas de histologia e microscopia de campo claro e *Light sheet* foram comparadas. A microscopia de fluorescência *Light Sheet* foi usada para comparação histológica do tecido cardíaco de diferentes linhas transgénicas e entre modelos de regeneração.

Com o presente trabalho, foram estabelecidas as metodologias inovadoras propostas, não implementadas anteriormente no Instituto de Medicina Molecular (iMM). Obtiveram-se também resultados preliminares que demonstram diferenças na morfologia do enfarte entre modelos de reparação bem como concentrações elevadas de sCD40L no modelo de reparação cardíaca exposto a imunossupressores.

Palavras-chave: Regeneração, peixe-zebra, inflamação

ABSTRACT

Myocardial Infarction (MI), or heart attack, is an important clinical condition. After a MI, the human heart is unable to regenerate and further complications leading to heart failure can occur.

Zebrafish (*Danio rerio*) has the ability to regenerate up to 25% of cyocauterized ventricle. The fish retains a high homology with humans, in terms of gene expression and electric heart activity, thus being a suitable model for heart repair studies.

Previous work from research group were the present thesis was conducted shown levels of soluble CD40 ligand (sCD40L), a transmembrane glycoprotein, associate with persistent endothelial dysfunction and compromised cardiac repair after-MI. Further mechanistic studies are mandatory to better understand association of sCD40L to heart repair, which can be achieved using zebrafish model.

This thesis objective was to establish protocols for evaluation of longitudinal variations of sCD40L after cryoinjury induced-MI alongside with myocardial repair in zebrafish. To achieve this objective, protocols of cryoinjury, blood collection, histology and microscopy were compared and optimized. Furthermore, the project also intended to implement a Compromised Regeneration/Immunosuppression Model. Prospectively, this dissertation can contribute to further studies in zebrafish that would provide translation for clinical research involving cardiac repair post-MI in human patients.

In this project, several innovative techniques were established. Also, preliminary results were obtained showing altered cardiac tissue histology and higher concentrations of sCD40L on fish of the Compromised Regeneration Model (with zebrafish exposed to immunosuppressors).

Key Words: Regeneration, zebrafish, inflammation, infarction.

INDEX

FIGURES INDEX

ABBREVIATIONS

3D – three-dimensional

3DISCO – 3D imaging of solvent cleared organs

AMI – acute myocardial infarction

BABB – benzyl-benzoate

BF – bright-field

CD40L – cluster of differentiation 40 ligand

cmlc2 – cardiac myosin light chain 2

CTR – control group

CUBIC – clear unobstructed brain imaging cocktails and computational analysis

DA – dorsal aorta

DGAV – Direcção Geral de Alimentação e Veterinária

DiI – 1,1'-dioctadecyl-3,3,3',3'-tetramethylindocarbocyanine perchlorate

DMSO – dimethylsulfoxide

dpi – day(s) post-injury

ECs – endothelial cells

ELISA – Enzyme-Linked Immunosorbent Assay

eNOS – endothelial nitric oxide synthase

FMUL – Faculdade de Medicina da Universidade de Lisboa

HF – heart failure

HRP - horseradish peroxidase

iDISCO – immunolabeling-enabled three-dimensional imaging of solvent-cleared organs

iMM – Instituto de Medicina Molecular

LAS – Leica Acquisition Suite

LSFM – light sheet fluorescence microscopy

MI – myocardial infarction

MMPs – matrix metalloproteinases

NT-proBNP – N-terminal pro-brain natriuretic peptide

OCT – optimal cutting temperature

OD – optical density

PACT – passive clarity technique

PARS – perfusion-assisted agent release in situ

PBS – phosphate-buffered saline

PCV – posterior cardinal vein

PFA – paraformaldehyde

RT – room temperature

sCD40L – soluble cluster of differentiation 40 ligand

SMCs – smooth muscle cells

TDE – 2,2′-thiodiethanol

TNF – tumor necrosis factor

VEGF – vascular endothelial growth factor

INTRODUCTION

MYOCARDIAL INFARCTION| HEALING AND REMODELING IN MAMMALS

Rupture or erosion of an atherosclerotic plaque are particularly frequent, clinically relevant, 'wounds' regarding the cardiovascular system. Most common consequence of those lesions is a myocardial infarction (MI) (Frantz et al., 2009).

Cardiovascular diseases have long been the leading cause of morbidity and mortality worldwide, among which, MI, generally known as a heart attack, is associated with the highest risk of death and other complications (Chablais et al., 2011; Huang et al., 2013). Clinically, MI can be defined as "necrosis of cardiac myocytes caused by prolonged ischemia" in consequence of a blood supply disruption to the injured area (Alpert et al., 2000; Huang et al., 2013).

As a consequence of an atherosclerotic plaque (consisting of lipids, cholesterol, fatty acids and white blood cells, primarily macrophages) growth, plaque rupture or erosion can occur, leading to thrombus formation and subsequent obstruction of a coronary artery. Resulting blockage restricts blood flow to myocardium (ischemia), impairing energy metabolism and reducing infarcted area oxygenation, thus triggering cardiomyocyte death (necrosis) (Betts et al., 2013; Chablais et al., 2011; Frangogiannis et al., 2002; Huang et al., 2013).

In surviving patients, as the mammalian heart is incapable of significant regeneration – cardiomyocytes are terminally differentiated and unable to divide –, dead myocardium is, eventually, healed and replaced by a collagen-rich scar tissue (Chablais et al., 2011; Lien et al., 2012; Major and Poss, 2007). This considered, infarct size is then dependent on myocardial region supplied by infarct-related coronary artery (McKay et al., 1986).

Healing process is first dominated by inflammatory response (degradation of extracellular matrix, inhibition of tissue proliferation, and release of inflammatory

mediators, known as 'inflammatory phenotype') and then turn to repair (increased matrix synthesis, proliferation of fibroblasts and inflammatory cells, and release of fibrosis promoting cytokines leading to scar formation, identified as 'activated phenotype') (Frantz et al., 2009).

After cardiomyocyte death, and with some feasible time overlap, inflammatory cells invade the infarct region and, somewhat later, myofibroblasts, responsible for reconstruction of a new collagen network, appear in the wound. Increased activities of collagenases, and other neutral proteinases, have been nominated responsible for rapid degradation of extracellular matrix collagen in MI. Actions of myofibroblasts are systematic, and crucial, for scar formation under difficult condition of heart's rhythmic contraction. After several weeks, a solid scar has appeared with a stable collagen structure, overall little cellularity, but with some myofibroblasts remaining in the tissue (Willems et al., 1994). Hence, healing is a complex process of invasion, transformation and apoptosis of various cell types, which is highly regulated (Ertl and Frantz, 2005).

In early post-infarction period, the scar provides mechanical support to infarcted heart, being vital to prevent myocardial wall rupture. Nevertheless, scarring progressively leads to profound changes in ventricular architecture and geometry, referred to as 'ventricular remodeling', causing loss of myocardium's contractility, which can ultimately lead to further cardiac complications, as heart failure (HF) (Ertl and Frantz, 2005; González-Rosa et al., 2011).

MYOCARDIAL INFARCTION| HEART REGENERATION IN ZEBRAFISH (*Danio rerio*)

In contrast to mammals, whose limitation in terms of cardiac regenerative potential is the inability of adult cardiomyocytes to re-enter cell cycle, other vertebrates, such as teleost fish like zebrafish, have the aptitude to reconstitute injured myocardium with little to no scarring (Chablais et al., 2011; González-Rosa et al., 2011). Zebrafish can

also regenerate many other organs and tissues, such as fin, optic nerve, liver, retina and spinal cord (Poss et al., 2003).

To date, it has been shown that adult zebrafish heart is able to completely regenerate after injury caused by cryocauterization of 25% of the ventricle, as well as resection of up to 20% of the ventricle in 1–2 months (Chablais et al., 2011; González-Rosa et al., 2011; Poss et al., 2002). It was described that both ventricular resection and cryoinjury induced lesions are repaired using similar cellular mechanisms, with only a few temporal differences, but cryocauterization produces an injury most akin to cardiac tissue damage seen in human patients after a myocardial infarction (Schnabel et al., 2011).

Injuries are followed by complete regeneration of myocardium, endocardium and coronary vasculature, which happens through massive cell proliferation at injury site, overcoming scar formation, and allowing cardiac muscle to fully regrow (González-Rosa et al., 2011; Poss et al., 2002).

Cellular and molecular events during heart regeneration in zebrafish can be divided in three overlapping phases: (i) resolution of inflammation, where infarct is cleared from dead cells by macrophages; (ii) reparative phase, with formation of a fibrin layer that seals the wound, and accumulation of fibroblasts that produce a collagen frame; and finally, (iii) regenerative phase, unique to zebrafish, where pre-existing cardiomyocytes undergo limited dedifferentiation, and proliferate to replace lost myocardium (Chablais et al., 2011; Jopling et al., 2010; Lien et al., 2012). Also during regeneration, epicardium is activated by re-expressing embryonic markers and can contribute to coronary vessel formation that vascularizes regenerated tissues. Endocardium is likewise activated and supports cardiomyocyte proliferation (Kikuchi et al., 2011).

Moreover, capillaries have been detected emerging from border zones and invading the injured area, suggesting a directed migration towards damaged tissue.

Angiogenesis, therefore, seems to be fundamental to restore interrupted blood flow (González-Rosa et al., 2011).

As shown in literature, tissue repair in zebrafish can be compromised by manipulating its immune response, which might comprise diminished phagocytes recruitment, angiogenesis, cell proliferation and inhibition of neutrophil migration (Chatzopoulou et al., 2016; Huang et al., 2013). Furthermore, inhibition of immune response, in zebrafish, leads to excess collagen deposition in the wound, supporting prevailing hypothesis that scar formation opposes regeneration during cardiac repair in mammals (Rasmussen et al., 2011).

sCD40L

Healing after a MI is composed of various stages, including release of inflammatory mediators, such as CD40L (Frantz et al., 2009).

CD40 ligand (CD40L or CD154), is a type II transmembrane glycoprotein, with a molecular weight between 32 and 39 kDa (van Kooten and Banchereau, 2000). CD40L is a member of tumor necrosis factor (TNF) superfamily and expressed primarily by activated T cells, as well as activated B cells and platelets; under inflammatory conditions is also induced on mast cells, basophils, monocyte cells, and natural killer cells (Armitage et al., 1992; Carbone et al., 1997; Gauchat et al., 1993; Karpusas et al., 1995; Lederman et al., 1992).

As its name suggests, CD40L binds to CD40, establishing a system that seems to play an important role, not only in cellular immunity and inflammation, but also in pathophysiology of atherosclerosis (Bonnefoy and Noelle, 1994; Laman et al., 1997). This system has shown expression in nonhematopoietic cells as well, including endothelial cells (ECs), fibroblasts, smooth muscle cells (SMCs), and platelets (Henn et al., 2001; Mach et al., 1997). Binding of CD40 to these cell types induces a proinflammatory and prothrombotic response, as evidenced by the release of inflammatory cytokines,

expression of adhesion molecules, activation of matrix metalloproteinases (MMPs), and procoagulant tissue factor (Urbich et al., 2002).

A soluble form of CD40L (sCD40L), with TNF homology region fully preserved, was reported to express activities similar to its transmembrane form, like bind to CD40 and replace $CD40L^{+}$-T cells in activation of B cells, among others (Graf et al., 1995; Mazzei et al., 1995).

Correlation between sCD40L and lower vasculature dysfunction suggests that increased sCD40L levels in heart HF could reflect other pathogenic mechanisms in myocardial failure, including activation of MMPs, and induction of inflammatory cytokines and chemokines. Whatever the mechanisms, CD40-expressing cardiomyocytes may directly interact with CD40L, contributing to persistent tissue inflammation and remodeling within failing myocardium. These findings, suggest enhanced release of sCD40L within coronary circulation, further supporting enhanced CD40/CD40L interaction within myocardium (Santilli et al., 2007).

High levels of sCD40L have also been associated with increased cardiovascular events in women (Schönbeck et al., 2001). Previous results obtained by the research group were the present work was conducted, demonstrated a relation between time changes of sCD40L over 1 month after myocardial infarction onset and markers of endothelial and vascular function (G894T eNOS polymorphism and VEGF concentrations, which may propose a role of sCD40L in angiogenesis), but not to the platelet CD62P expression, which might suggest that, along the disease progression in acute myocardial infarction (AMI) patients, sCD40L is not related to platelet activation or thrombosis (Napoleão et al., 2015).

More recently, it was also shown that lower levels of sCD40L over 30 days after MI onset seem to be associated to endothelial dysfunction and to impaired myocardial repair post-MI. This was inferred by the connection of sCD40L with markers of endothelial dysfunction (G894T endothelial nitric oxide synthase - eNOS polymorphism),

vascular function (vascular endothelial growth factor - VEGF), left ventricular dysfunction (N-terminal pro-brain natriuretic peptide - NT-proBNP) and with a specific profile of miRNA expression related to cardiac injury and dysfunction (Napoleão et al., 2016).

Though there are studies implicating CD40L/sCD40L in endothelial dysfunction and angiogenesis, no information has been obtained, so far, on how sCD40L is related to myocardial repair post-cardiac injury (Henn et al., 1998; Urbich et al., 2002; Chen et al., 2008; Hristov et al., 2010).

OBJECTIVES

This thesis aimed to establish protocols for evaluation of longitudinal variations of sCD40L after cryoinjury induced-MI alongside with myocardial repair in zebrafish. To achieve this objective, protocols of cryoinjury, blood collection, histology and microscopy were compared and optimized.

Furthermore, the project also intended to implement a Compromised Regeneration/Immunosuppression Model, in which fish are exposed to an immunosupressor that compromises cardiac regeneration, which was used to provide comparable results to those obtained with a Normal Regeneration Model, in terms of sCD40L concentrations, histology and mortality.

Prospectively, this dissertation can contribute to further studies in zebrafish that would provide a better extrapolation for clinical research involving cardiac repair post-MI in human patients.

MATERIAL AND METHODS

STUDY MODEL| ZEBRAFISH (*Danio rerio*)

Different from a four-chambered human heart, zebrafish (*Danio rerio*) heart is a simple two-chambered structure, composed of one atrium and one ventricle (Fig.1a). Despite the anatomical difference (Fig.1b), numerous studies have shown that embryonic morphogenesis, essential genes expression programming, and electrical activity of human and zebrafish hearts are highly analogous, making zebrafish a suitable model organism to study cardiac development and related human diseases, such as MI (Bakkers, 2011).

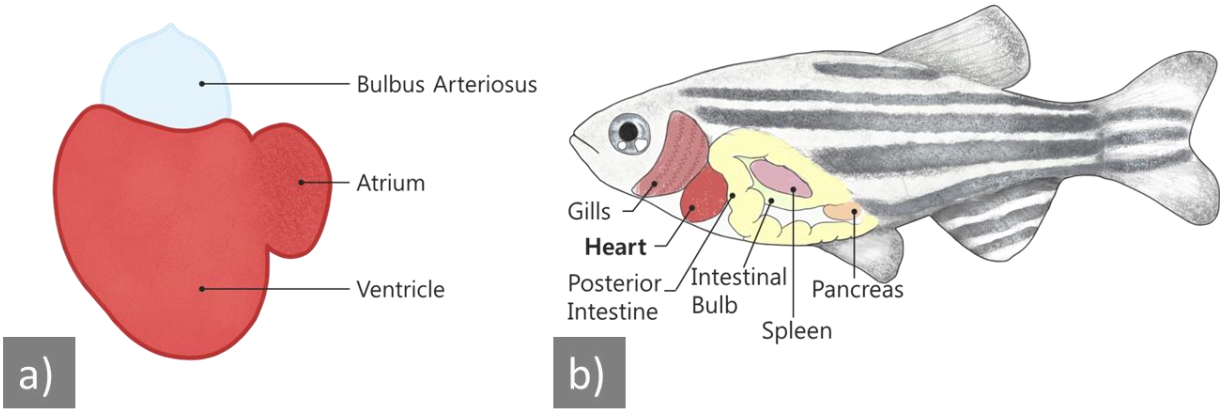

Fig. 1. Schematics of Zebrafish simplified anatomy. Heart anatomy (a) and full body with labelled structures (b).

- **Zebrafish husbandry**

Regeneration posterior to MI in zebrafish was assessed through usage of the *Tg(fli1a:EGFP)* transgenic line marked for blood and lymphatic vessels' ECs, which allows imaging of vessel formation (Lawson and Weinstein, 2002). Evaluation of cardiac tissue histology between transgenic lines was done comparing several transgenic lines:

- *Tg(nestin-cre:GFP)* – described in mice as marking central and peripheral nervous system and a few isolated kidney and heart cells, cardiomyocytes (Kachinsky et al., 1995);

- *Tg(ras:EGFP)* – marks cellular membrane (Chi et al., 2008);

- *Tg(kdrl:ras-cherry)* – like *Tg(fli1a:EGFP)* marks ECs, but only of blood vessels (Cross et al., 2003);

- *Tg(cmlc2:GFP)* – specific for heart muscle cells, cardiomyocytes (Huang et al., 2003).

In this thesis, a total of 144 fishes were used.

- **Ethical issues**

All the experiments were conducted according to the directives of Direcção Geral de Alimentação e Veterinária (DGAV) (PORT1005/92) and after approval by the Animal User and Ethical Committees of the host insitutuion, Faculdade de Medicina da Universidade de Lisboa (FMUL), and also of Instituto de Medicina Molecular (iMM) were the Zebrafish Facility is installed (Project Approved 04021/000/000/2016).

Furthermore, the Principle of the Three R's was applied. For example, fish of *Tg(nestin-cre:GFP)*, *Tg(ras:EGFP)* and *Tg(kdrl:ras-cherry)* transgenic lines were already to be sacrificed by fish-facility staff.

ANIMAL PROCEDURES

- **Cryoinjury procedure**

Cryoinjury is the injury type most alike to cardiac tissue damage seen in human patients, when compared to ventricular resection (Schnabel et al., 2011).

Herein, cryoinjury was performed based on the protocol previously described by González-Rosa and Mercader (2012), in adult zebrafish ageing between 1 and 2 years raised at a density of 3 fish/L. For this, fish were anesthetized for no more than 4 minutes (depending on fish size and weight) in 0.04% tricaine (Sigma Aldrich), measured (from snout to tail-end) and placed ventral up into a very soft sponge (Fig. 2a). With tweezers, the skin was pinched up just above the heart and cut it with scissors, exposing the ventricle which was readily frozen by applying, until thawing, a hand-made cryoprobe

previously immersed in liquid nitrogen (Fig. 2b-d). Fish are revived soon after the procedure by gently pumping water into the gills with a pipette (Fig. 2e).

Thereafter, animals were placed into small tanks with a middle divisor (2 per tank, accordingly identified), that then stay in a temperature-controlled bath until their sacrifice.

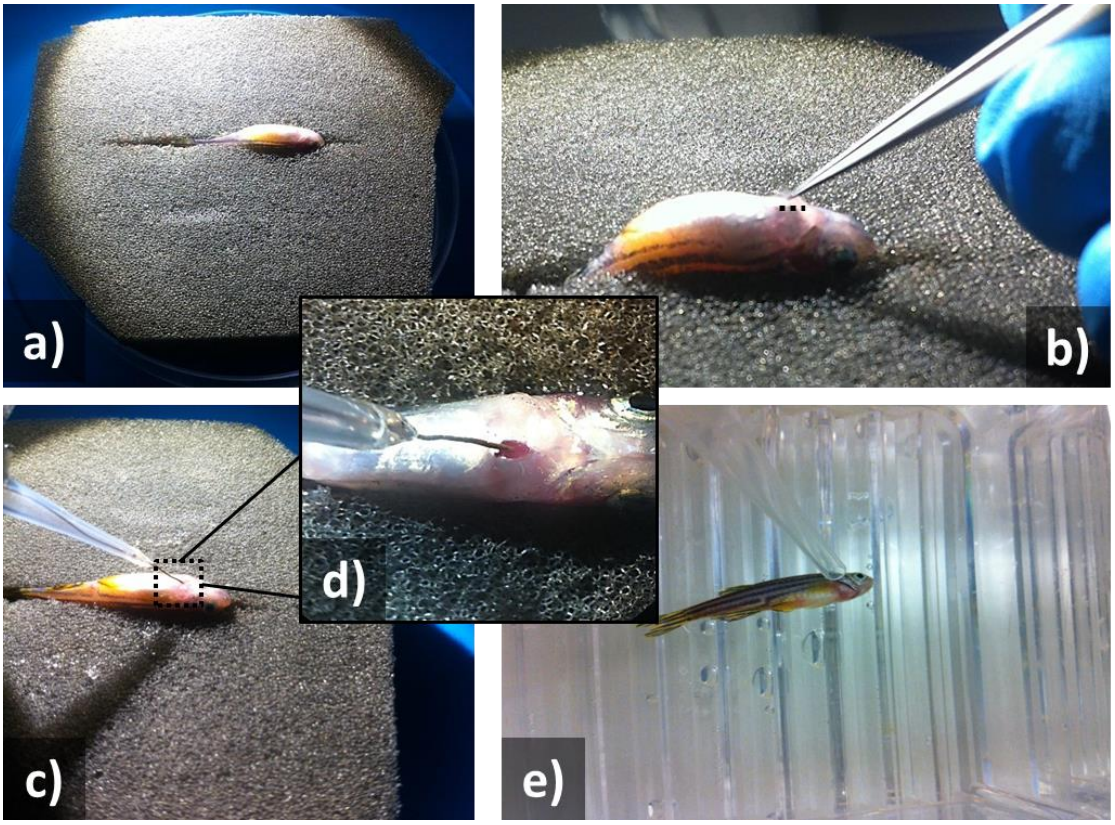

Fig. 2. Illustrative snapshots of cryoinjury procedure. Fish was placed ventral up into a very soft sponge (a). With tweezers, the skin was pinched just above the heart and cut with scissors – along dotted line (b). The cryoprobe, previously immersed into liquid nitrogen, was applied on the exposed heart until thawing (c-d). Lastly, fish was revived by gently pumping water into gills with a plastic pipette (e).

This procedure, cryoinjury, was considered by the ethical commission at DGAV as Moderate, since this is not a terminal procedure and fish recover fast with no compromise of swimming ability.

Assessment of injury's presence was done 2 hours' post-infarction (to allow wound stabilization) through fluorescence stereo microscope Zeiss Axio Zoom V16 with a

monochromatic camera (AxioCam MRm), using Zeiss's Zen 2012 (Blue Edition) acquisition software. This was done by observing the non-fluorescent (necrotic) area (Fig. 3).

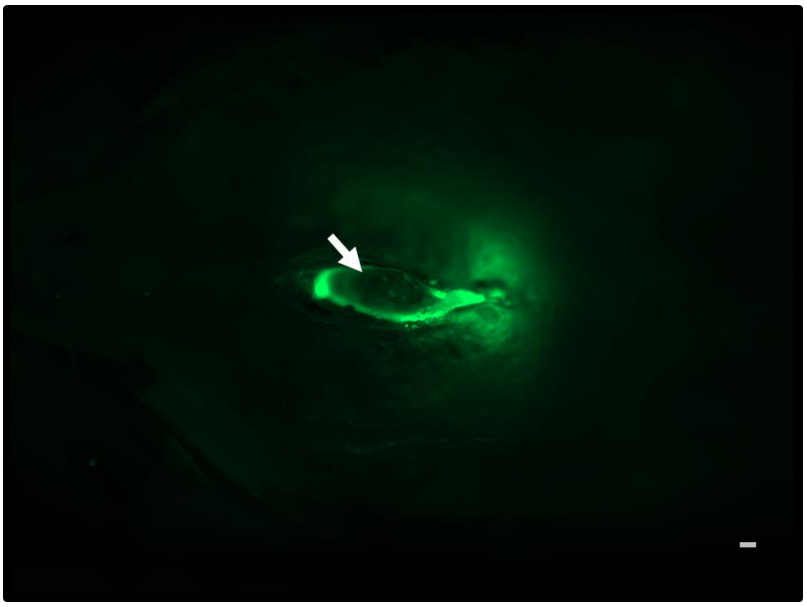

Fig. 3. Snapshot of injured heart 2 hours' post-infarction taken in Zeiss Axio Zoom V16 microscope. Fish belongs to *Tg(cmlc2:GFP)* transgenic line. Infarcted area (white arrow) without fluorescence. Scale bar: 100 μm.

Control fishes were not submitted to cryoinjury (without exposure of ventricle).

Animals were sacrificed at different times post-injury. Anaesthesia was performed by immersing fish in 0.04% tricaine, previous to blood and heart collection. Evaluation of cardiac repair post-injury and of sCD40L was performed on following time-points: 1-day post-injury (dpi), 3, 7 and 21 dpi, which mark important regeneration events, respectively: endocardium activation; inflammation; epicardium activation and fibroblast proliferation; and cardiomyocyte proliferation plus neovascularization, followed by collagen scarring (Lien et al., 2012).

- **Immunosuppression assay**

Huang *et al*. showed immunosuppression, by treatment with glucocorticoid, effectively delays cardiac repair in adults (Huang et al., 2013). Thus, in the present study, this model of immunosuppression was used as a model of impaired repair after cardiac injury.

Here, adult zebrafish were exposed to water containing 0.25 μM beclomethasone (Fluka) from 24 hours prior to cryoinjury until sacrifice for blood collection and heart dissection (Huang et al., 2013). Water was changed every day until 3 dpi, to avoid infection, and after that was changed with a 1-day break.

All water changing procedures in this assay were done in the quarantine, where fish were being held until their sacrifice.

Blood Collection

Blood collection in zebrafish is a rather strenuous task, demanding thorough training, since fish are small and their blood is prone to coagulation and hemolysis. Hence the existence of numerous different methods, with varying success, depending blood usage (like glucose measurements, serum analysis, etc.) and whether the procedure is terminal or not.

Techniques used so far in research comprise: retro orbital extraction (Vliegenthart et al. 2014); extraction through decapitation (Eames et al. 2010), and tail amputation (Pedroso et al., 2012); whole animal centrifugation with its tail amputated (Babaei et al., 2013); collection from aorta through a dorsal cut at dorsal fins' posterior region (Jagadeeswaran and Sheehan, 1999); collection from dorsal aorta (DA) and posterior cardinal vein (PCV), adjacent to the animal's spine at caudal region – this method was designed for longitudinal studies, allowing several collections from the same fish (Zang et al., 2015); and collection from abdominal region.

From the previously described, for effectiveness evaluation, since at the iMM there was no blood collection method established, two methods were chosen for further comparison: collection from abdominal region; and collection from caudal region. Both were elected based, respectively, on their placement suitability and advantage of collecting blood directly from the dorsal aorta and posterior cardinal vein. Cardiac

puncture could not be applied since it destroys the heart's structure, which would be needed for histology methods.

- **Blood collection protocol – Abdominal region**

Blood collection from abdominal region starts with a previously cryoinjured, and anesthetized, animal placed ventral up in a soft sponge (Fig. 4a). Heart was exposed by cutting the skin (noting that sometimes, blood could start to pour out immediately) (Fig. 4b-c). After heart dissection and storage, with consequent bleeding, the most amount of blood possible was collected into a previously heparinized capillary (which should be heparinized at least 2 hours prior to blood collection) inserted in a suction tube) (Fig. 4d-f).

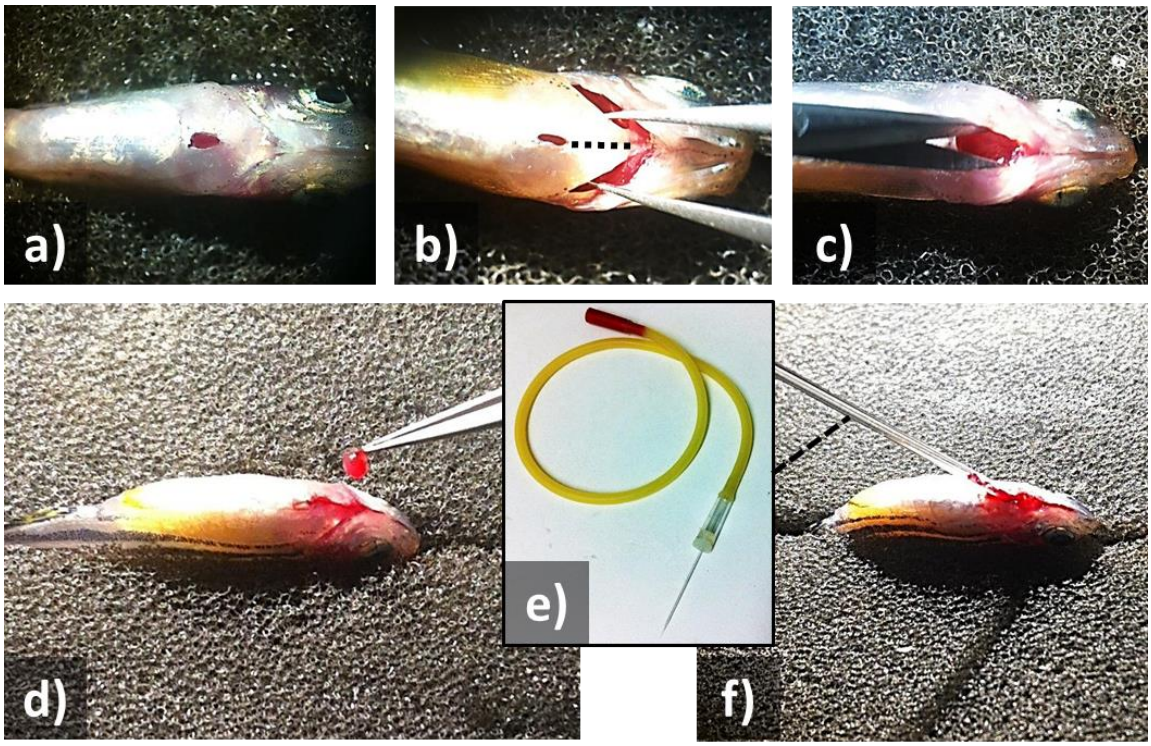

Fig. 4. Illustrative snapshots of blood collection from abdominal region procedure. At sacrifice time-point, a previously cryoinjured animal was placed ventral up in a soft sponge as previously described (a), brachial area was secured with tweezers, and cut along the dotted line with scissors (b). Fish was opened (c) and the heart removed and stored (d). Then, the maximum amount of blood that came out was rapidly collected (f) with a capillary inserted into a suction tube (e).

- **Blood collection protocol – Caudal region**

For this procedure, the animal should be deeply anesthetized and placed laterally with its anterior section secured with a small, dry paper tissue (Fig. 5a).

According to the method described by Zang *et al.*, a heparinized capillary (introduced into the contraption described and displayed above, with its tip cut diagonally to facilitate insertion) was inserted alongside the body's axis, posterior to the anus, where dorsal aorta DA and PCV are located, just ventral to the spine. Using an imaginary line that begins at the animal's tail 'V', the capillary tip was inserted in such way that it touches its spine right away and then moved slightly downward. Blood started to upsurge right away, and just a gentle pull through the mouthpiece was necessary to help it rise until no more came out (Zang et al., 2015) (Fig. 5b-c). In this step, it is important to be cautious of not removing the capillary while sucking, in order to prevent blood's sudden rise, which can lead to hemolysis.

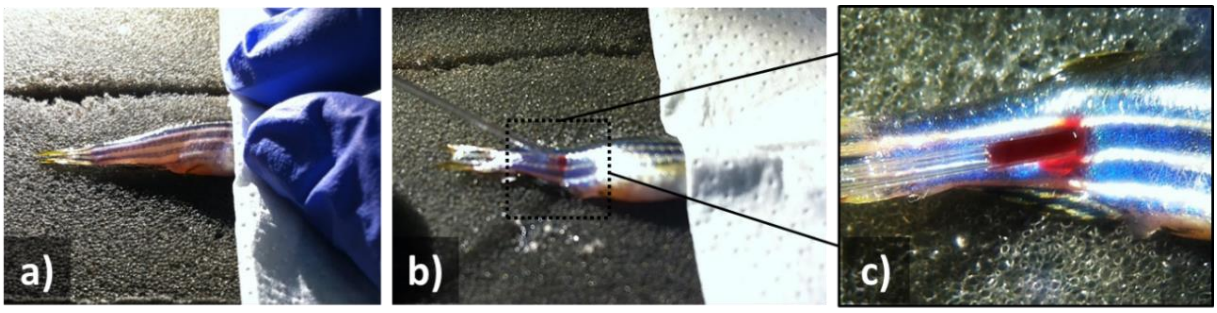

Fig. 5. Illustrative snapshots of blood collection from the caudal region procedure. After anesthesia, the animal was placed laterally and secured with a small, dry paper tissue (a). A capillary was inserted along the lateral line in order to touch the fish's spine, and then relocated slightly ventral to reach the dorsal aorta (b). Afterwards, blood started to pour into the capillary (c).

- **Blood centrifugation protocol**

Blood collected, independently of which method was used, was drawn to a microtube with 5 µL of saline solution at room temperature (RT). To minimize hemolysis, samples were centrifuged within 10 minutes upon collection, for 15 minutes at 13750 *g*. After centrifugation, serum (supernatant) was quantified using a micropipette, collected and stored at -20°C, for a maximum of 2 months.

HISTOLOGY PROTOCOLS

- **Heart dissection**

Whole zebrafish hearts were dissected and processed for histological analysis (see below). Heart dissection begins equally to blood collection from abdominal region procedure, with the fish anesthetized and placed ventral up in a soft sponge (Fig. 6a). A cut exposing the heart was made with scissors and with tweezers providing support by securing the branchial area (Fig. 6b). After the cut was made, surgical scissors were used to keep the heart cavity open in order to help reach the bulb. Its tip was seized with a tweezer and pulled gently, with extreme care so not to separate the bulb from the ventricle (though the bulb is not the main area of focus, it allows to distinguish the heart's apical-basal orientation) (Fig. 6c-d). Collected hearts are, thereafter, placed in a 1 mL microtube containing 300 µL of 4% paraformaldehyde (PFA; Merck Millipore) and stored at 4ºC.

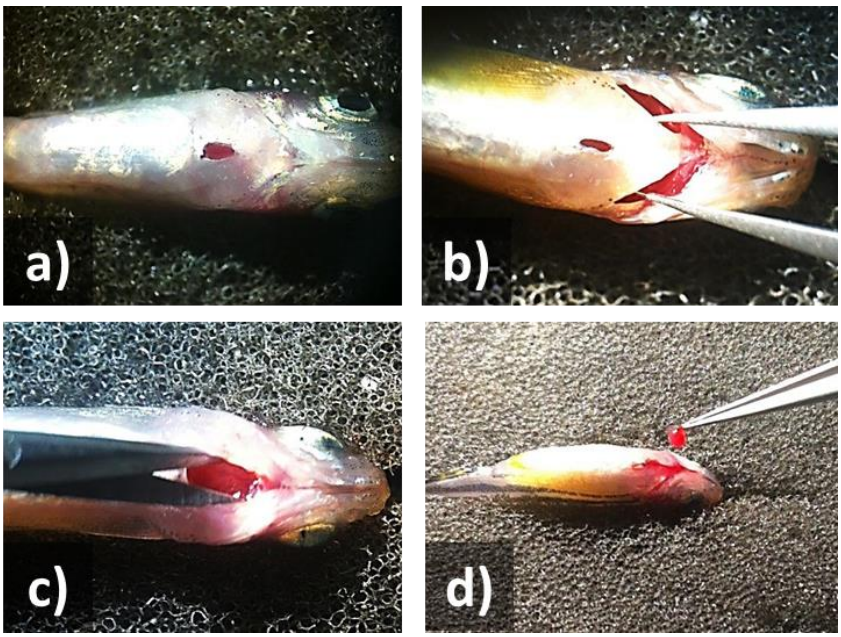

Fig. 6. Illustrative snapshots of heart dissection procedure. Procedure of heart dissection (a-d) is followed through as described in the previous figure 4, steps a-d.

- **Histological techniques**

In general, most biological tissues have very little contrast, being difficult to distinguish cellular details, and thus, sections need to be stained to allow that distinction

by developing specific colors. One of the most widely used histologic techniques for morphological evaluation, Hematoxylin and Eosin staining is the primary diagnostic technique used in a histopathology laboratory, first used in 1896 by Paul Mayer, it uses two separate dyes, one staining the nucleus and the other staining the cytoplasm and connective tissue (Cook, 1997; Mescher, 2013). Hematoxylin is a dark purple dye, with affinity with basophilic substances, that will stain the chromatin (nuclear material) within the nucleus, leaving it a deep purple-blue color. Eosin is a pink to red dye, with affinity with acidophilic substances, staining cytoplasmic material, including connective tissue and collagen, in a pink-red counterstain (Mescher, 2013; Peckham, 2011).

For Hematoxylin and Eosin staining, hearts were immediately immersed in 10% neutral-buffered formalin. Samples were embedded in optimal cutting temperature (OCT) within a cryo-mold, frozen in liquid nitrogen-cooled isopentane, cryosectioned longitudinally (LEICA CM 3050S) and stained with hematoxylin and eosin. Sections were cut at the thickness of 6 μm and 10 μm.

- **Clearing protocols**

Optical clearing aids optical sectioning by increasing tissue transparency so that the specimen has a uniform refractive index throughout its form, to minimize light scattering (where light rays that should travel in straight lines are reflected off of molecules, membranes, organelles, and cells in the tissue; and deviated many times) and allow its proper imaging (Hama et al., 2011; Richardson and Lichtman, 2015). Numerous clearing solutions have been created, used mainly in neurosciences, and can be divided into two main categories, tissue dehydration and solvent-based clearing; and aqueous-based techniques (comprising simple immersion, hydrogel embedding and hyperhydration) (Richardson and Lichtman, 2015).

Solvent-based clearing started in 1914 with Spalteholz (Richardson and Lichtman, 2015), and includes benzyl-benzoate (BABB) (Dodt et al., 2007), 3D imaging of solvent

cleared organs (3DISCO) (Ertürk et al., 2012), and immunolabeling-enabled three-dimensional imaging of solvent-cleared organs (iDISCO) (Renier et al., 2014).

Simple immersion, belonging to aqueous-based clearing techniques, includes the largest array of solutions to date. FocusClear (Chiang et al., 2002; Chien and Chiang, 2003; Lin et al., 2007), 2,2′-thiodiethanol (TDE) (Staudt et al., 2007; Aoyagi et al., 2015; Costantini et al., 2015), sucrose and Triton X-100 solution (Tsai et al., 2009), Clear^{T} and Clear^{T2} (Kuwajima et al., 2013), SeeDB and SeeDB2 (Ke et al., 2013, 2016), and FRUIT (Hou et al., 2015).

Hydrogel embedding techniques so far include CLARITY (Chung et al., 2013), passive clarity technique (PACT) and perfusion-assisted agent release in situ (PARS) (Yang et al., 2014).

Solutions based on hyperhydration – where the sample is immersed an aqueous solution and allowed to passively clear – include clear unobstructed brain imaging cocktails and computational analysis (CUBIC) (Susaki et al., 2014; Tainaka et al., 2014), Sca*l*eA2 (Hama et al., 2011) and Sca*l*eS (Hama et al., 2015). Sca*l*e protocol was chosen for sample clearing due to its financial constraints, as CUBIC is a reagent bought already prepared, and is therefore more expensive than Sca*l*e, which can be made at the laboratory; and due to it being made specifically for clearing tissues while conserving fluorescent signaling (which is crucial in this work). Sca*l*eA2 and Sca*l*eS, whose refractive index match that of the microscope objective used (1.45±0.03), were chosen to compare which provided the best clearing results. Sca*l*eA2, was reported to successfully clear slices and whole mouse brain as well as mouse embryo, being more permissive to light than phosphate-buffered saline (PBS), 60% sucrose/PBS and FocusClear (Hama et al., 2011). Sca*l*eS efficiently cleared whole mouse brain and microglia plaques, being faster than Sca*l*eA2, free from tissue deformity problems, preserves immunostaining and 1,1'-dioctadecyl-3,3,3',3'-tetramethylindocarbocyanine perchlorate (DiI) labeling signals, and

according to the authors, seems to provide a better clearing than Sca*l*eA2, Clear$^{T/T2}$ and SeeDB (Hama et al., 2015).

ㄴ Clearing protocol – Sample fixation

Both clearing protocols (Sca*l*eA2 and Sca*l*eS) start with a fixation process. Briefly, immediately after dissection, as described above, hearts were fixed and stored at 4°C in 300 µL of 4% PFA, for at least 24h, protected from luminous sources.

ㄴ Clearing protocol – ScaleA2

Adapted Sca*l*eA2 protocol consists of eight different procedures as follows:

- Fixation (as described above);

- Adaptation/cryoprotection in PBS 20% sucrose (Merck Millipore; **300 µL**) for 20 hours at 4ºC in orbital shaker;

- Adaptation/wash in PBS (**300 µL**);

- Adaptation/refixation in 4% PFA (**300 µL**) for 1 hour at RT;

- Clearing in Sca*l*eA2 solution (10% w/v glycerol, Merck Millipore; 4 M urea, Merck Millipore; and 0.1% w/v Triton X-100, Merck Millipore; **300 µL**) at 37ºC, for approximately 2 weeks.

Mismatching refractive indexes of objective immersion and mounting medium can cause image degradation, expressed by z-axis stretching/compression that results in reduced axial resolution (Flood et al., 2013).

Due to Sca*l*eA2 solution having a refractive index of 1.378 (Hama et al., 2011), that mismatched that of the microscope objective used this project (see Microscopy section below) – with a refractive index of 1.45 (±0.03) –, a further procedure was added to the protocol to ensure transferring to a mounting solution of Sca*l*eS4(0), with a refraction index of 1.437 (Hama et al., 2011):

- Transferring scales/wash in PBS (**300 µL**);

- Transferring scales to Sca*l*eS4(0) (40% w/v D-sorbitol, Sigma Aldrich; 10% w/v glycerol,; 4 M urea; and 20% v/v dimethylsulfoxide – DMSO; **300 µL**);

- Mounting in Sca*l*eS4(0), noting that solution can last for up to two days.

- Clearing protocol – ScaleS

Adapted Sca*l*eS protocol also consists of eight different steps as follows:

- Fixation (as described above);

- Adaptation in Sca*l*eS0 (5% w/v glycerol; 20% w/v D-sorbitol; 1 mM methyl-β-cyclodextrin, Sigma Aldrich; 1 mM γ-cyclodextrin, Sigma Aldrich; 1% w/v N-acetyl-L-hydroxyproline, Sigma Aldrich; 3% v/v DMSO; PBS 1x; **300 µL**), for 12 hours at 37ºC;

- Permeabilization in Sca*l*eS1 (10% w/v glycerol; 20% w/v D-sorbitol; 4 M urea; 0.2% w/v Triron X-100; **300 µL**), for 12 hours at 37ºC;

- Permeabilization in Sca*l*eS2 (27% w/v D-sorbitol, 2.7 M urea, 0.1% w/v Triton X-100, 8.3% v/v DMSO; **300 µL**), for 12 hours at 37ºC;

- Permeabilization in Sca*l*eS3 (36.4% w/v D-sorbitol, 2.7 M urea, 9.1% v/v DMSO; **300 µL**), for 12 hours at 37ºC;

- Descaling in PBS (**300 µL**), for 12 hours at 4ºC;

- Clearing and mounting in Sca*l*eS4(0) (**300 µL**).

MICROSCOPY

- **Bright-field (BF) Microscopy**

BF microscopy is the most widely used, where stained preparations are examined by means of light passing through the specimen (Mescher, 2013).

For the purpose of histological heart sections observation, a Leica DM2500 microscope was used, with 10x and 20x objectives.

Images were acquired through Leica Acquisition Suite (LAS) software.

- **Light Sheet Fluorescence Microscopy (LSFM)**

Enhancement of high resolution optical methods for labeling, imaging and reconstruction of different cell populations, is important for Biological Research in order to better understand structure-function relationships in different intact tissues at three dimensions.

In LSFM the specimen is illuminated along a single plane with a sheet of light, typically generated via a set of illumination objectives (Huisken et al., 2004). This microscope employs optical sectioning which is a theoretically faster, simpler and more inexpensive alternative for three-dimensional reconstruction of fluorescently labeled structures at subcellular resolution, when compared with mechanical sectioning (Fig. 7a). Despite its usefulness, this has the set-back of tissue opacity, which can cause light scattering, that can be resolved with sample clearing (Hama et al., 2011). For this work, three-dimensional (3D) imaging of whole-mounted hearts was done in Zeiss Lightsheet Z. 1, LSFM microscope (Fig. 7b).

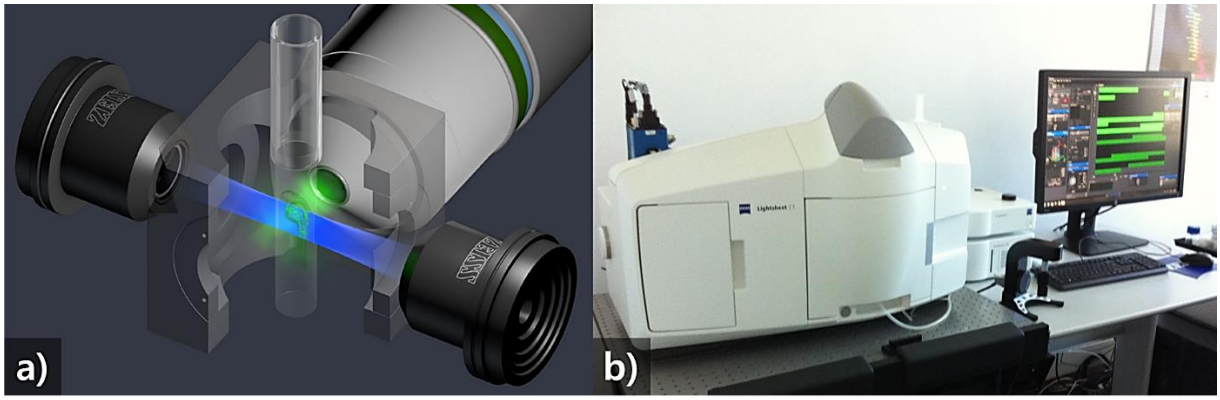

Fig. 7. Light Sheet Fluorescence Microscopy (LSFM). Schematic image of optical sectioning occurring in a LSFM (a) (Image Credit: Zeiss, 2016); and photograph of Zeiss Lightsheet Z. 1, LSFM microscope at iMM, on the left side on top of an anti-vibration platform, with assigned computer to the right.

Works using this type of microscopy, are particularly scarce, especially in Portugal, thus making it an extremely innovative tool for sample imaging.

ㄴ Light Sheet Fluorescence Microscopy (LSFM) - Sample mounting and visualization

In sample mounting, zebrafish heart was first placed into a petri-dish using a plastic Pasteur pipette with the tip cut-off. Excess mounting medium surrounding the heart was removed, with a smaller pipette, in order to leave the heart as dry as possible. Subsequently, the heart was super-glued, by its bulb, onto the tip of a plunger, placed inside a capillary introduced beforehand in sample-holding disk to be placed inside the microscope. Once sample-holding disk was inserted into microscope's motorized plate, it was lowered to the chamber containing the mounting medium used, Sca*l*eS4(0), immersing the sample.

Sample observation and image acquisition were performed using a 20x objective and Zen 2014 (Black Edition) software. Acquisition (taking from 1 to 3 hours, depending on heart dimension) was done in fields, together comprising whole heart area, with a varying number of optical slices per specimen (between 626 and 945, each with 1.646 μm thickness) which were later stitched and processed in Arivis Vision 4D software. Imaris software was subsequently used to further treat and compress 3D files.

ELISA ASSAY FOR SCD40L

Concentrations of sCD40L were measured in serum using a quantitative sandwich enzime-linked immunosorbent assay (ELISA) commercial kit (MyBioSource, Ref. MBS012099). Concentrations were expressed in ng/mL.

For sCD40L determination using the referred ELISA kit, 50 μL of serum is necessary for each well. Therefore, a pool of serum of 8 fish is needed to obtain that amount.

For 3 dpi, due to experimental constrains, the serum from the two models (normal and immunosuppression) were merged. This was an opportunity to test the possibility of dilute serum for sCD40L measurement. Therefore, two pools were used: pooled serum; and diluted (1:1) pooled serum.

ELISA assay was done according to manufacturer's instructions, as follows:

- Prepare wells (in duplicate with Standard, Sample and Blank/Control);

- Add Standard 50 µL to each Standard well, add Sample 50 µL to each Sample well, add Sample Diluent 50 µL to each Blank/Control well;

- Add 100 µL of horseradish peroxidase (HRP)-conjugate reagent to each well, incubate for 60 minutes at 37°C and wash the plate 4 times;

- Add Chromogen Solution A 50 µL and Chromogen Solution B 50 µL to each well, incubate for 15 minutes at 37°C;

- Add 50 µL Stop Solution to each well;

- Read the Optical Density (OD) at 450 nm within 15 minutes after adding Stop Solution.

RESULTS

COMPARISON OF BLOOD COLLECTION METHODOLOGIES

One of this thesis' aims was the optimization and comparison of different protocols for blood collection in order to establish the protocols that will be used in the future work studies by the investigation group at iMM.

Blood collection tests performed showed that less hemolysis was observed by using a capillary, when compared with fine p10 pipette tips, being dependent on whether the capillary tip was too fine, which would difficult blood expulsion into the microtube.

In terms of blood collection two methods were compared: collection from abdominal region; and collection from caudal region.

Collection from abdominal region is, overall, easier, requires less technical optimization, allows collection of a higher amount of blood, and is conveniently placed for heart dissection as blood was collected at sacrifice time points, with necessary heart dissection. However, hemolysis is more recurrent in this technique and more importantly, while collecting there is mixture of blood with other cavity fluids, contaminating it.

In order to use caudal area collection technique, it is necessary for the animal to be more deeply anesthetized (prolonged exposition to 0.04% tricaine) and required extra practice for blood collection to not move suddenly up and out of the capillary, since there is a higher pressure due to suction. There is a shorter amount of blood that can be collected, when compared with the previous technique, especially if the fish is substantially smaller in size or thinner in weight. Nonetheless, serum attained presents reduced hemolysis, meaning better sample quality for performing biochemical tests. Besides, there is no contamination of blood with other fluids from abdominal cavity. Thus, this was the chosen technique for blood collection in this work.

Comparison of Clearing Protocols

Comparison of Sca*l*e solutions represents an important step for the purpose of sample clearing, as it is needed to see which solution presents the best fit for what this work needs.

Theoretically, Sca*l*eA2 takes longer to get full sample clearing than Sca*l*eS, since in Sca*l*eS clearing progressively happens through solution change, and in Sca*l*eA2 clearing only happens when samples are immersed in Sca*l*eA2 solution for around a minimum of two weeks.

In this project, Sca*l*eS did not clear the zebrafish hearts, which were not transparent by the end of protocol. A prolonged exposition of hearts for two more days on Sca*l*eS4 was tried, however that procedure did not change the outcome.

An adaptation to Sca*l*eA2 protocol was applied as the hearts were incubated in Sca*l*eA2 solution at 37ºC, instead of RT (22-24ºC) referred by Hama et al (2011). This change allowed to shorten incubation period from more than 1 month to a minimum of 2 weeks (time until hearts were completely transparent). This method is time-consuming but in the end the hearts are fully transparent.

It is also noteworthy to mention that Sca*l*eS4 solution for mounting, common to both Sca*l*eA2 and Sca*l*eS protocols, was very difficult to make, as it always resulted very viscous in consistency and optically turbid, interfering with clear sample visualization on LSFM microscope. We found that Sca*l*eS4(0) not only is easier to attain, but remains translucent and has an almost identical refraction index (1.437) to Sca*l*eS4 (1.439), being appropriate to use as a mounting medium.

Comparison of Microscopy methodologies

- **Comparison of Microcopy Methodologies**

In this work, BF and LSFM microscopies were compared in terms of visualization quality for cardiac tissue injury.

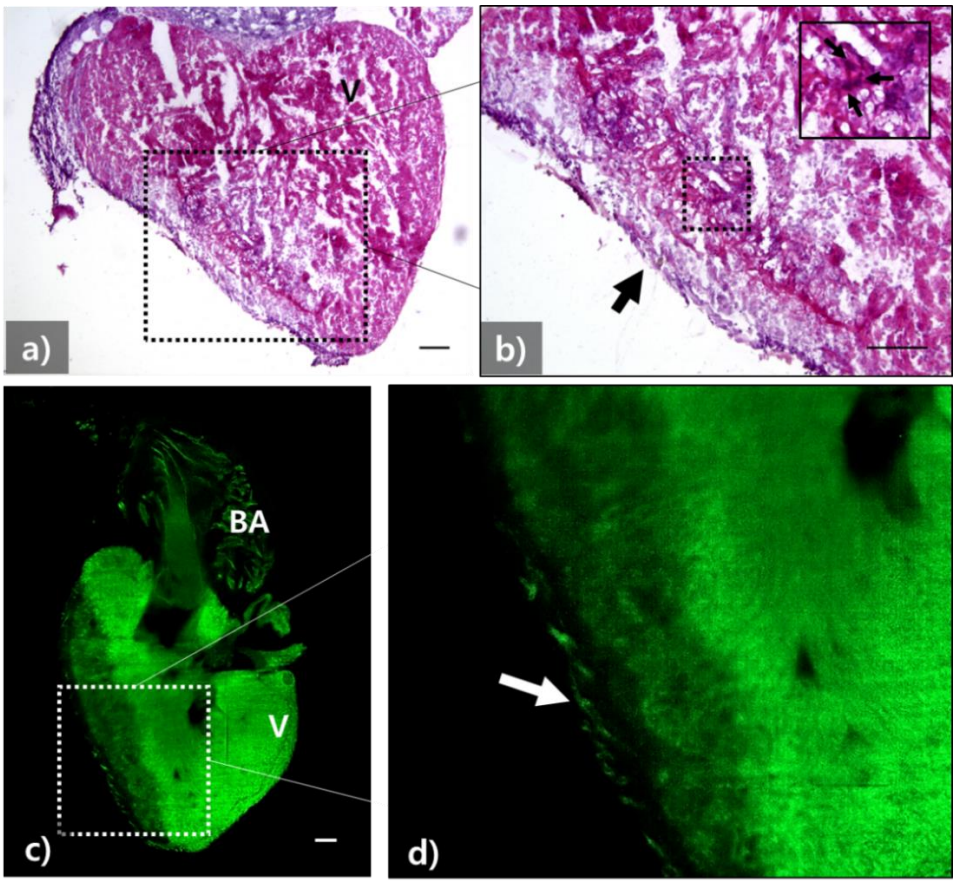

Fig. 8. Snapshots of cryocauterized hearts taken in BF and LSFM microscopes. Pictures of hearts at 3 dpi, one belonging to an unknown transgenic line (a), the other belonging to *Tg(Fli1a:EGFP)* (c). Small black arrows (b) point to inflammatory cells and bigger arrows (both black and white) point to thickened epicardium (b and d). BA stands for bulbus artriosus and V for ventricle. Scale bar: 100 µm.

BF microscopy, in this case allowed for a better observation of cardiac tissue morphology at injury site (its trabecular aspect, epicardium thickening and inflammatory cells) due to hematoxylin and eosin stain, that gives a better contrast between the tissue's different structures, not being specific for one cell-type (Fig. 8a-b).

LSFM, since it only shows the fluorescence visual information provided by the transgenic line used, *Tg(fli1a:EGFP)*, limits the amount of structures that are observed, in this case blood vessels. However, with this method it is easier to see the infarct shape due to clear contrast between infarct and remainder ventricle, making it better for measurements (Fig. 9e-f).

Infarct region (necrotic - no fluorescence area) and intact myocardium were also defined for the hearts above, and the areas were measured (Poss et al., 2002) using Fiji (Schindelin et al., 2012). Percentage of the infarct size relative to the entire ventricle was then calculated (as seen in Fig. 9).

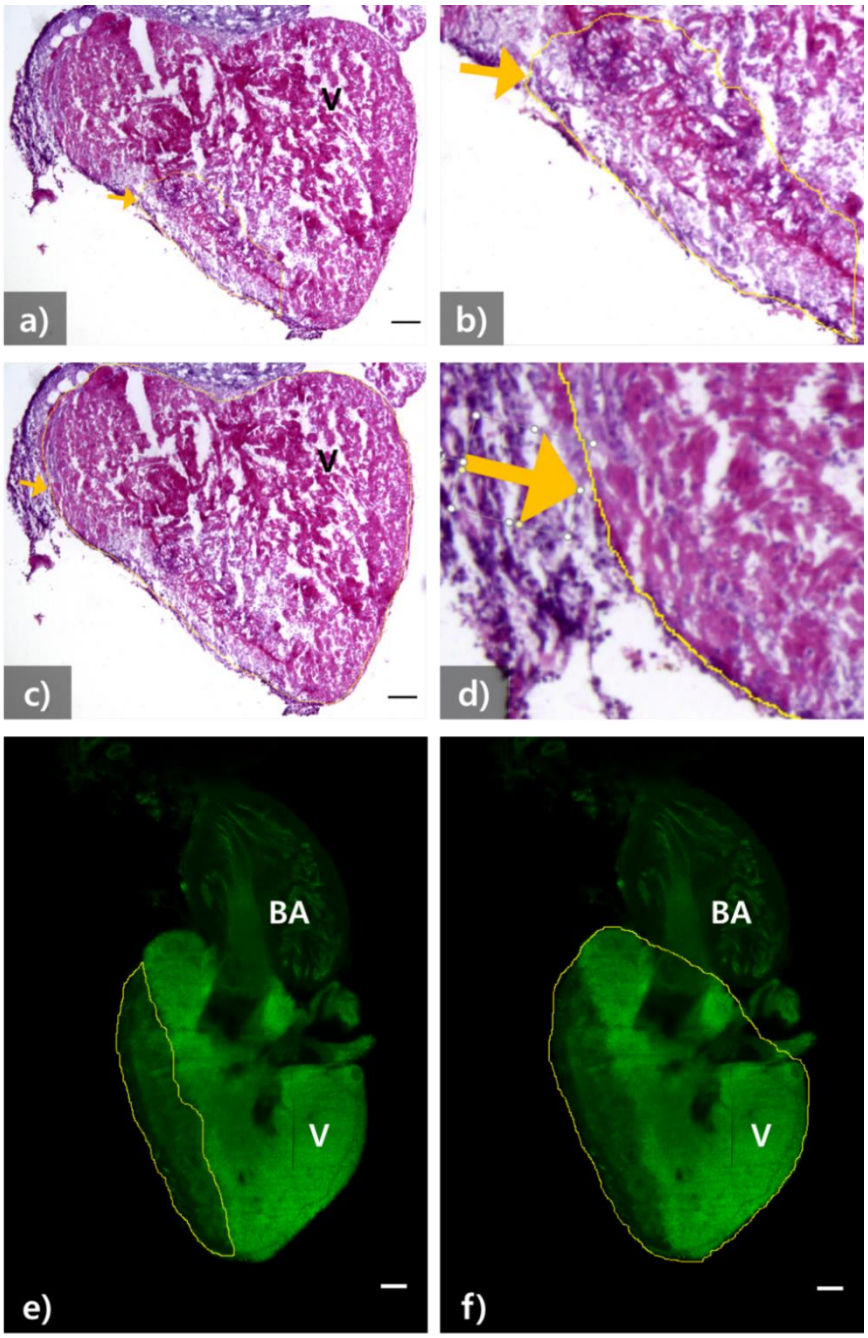

Fig. 9. Snapsots cryocauterized hearts taken in BF and LSFM microscopes for infarct percentage assessment. Pictures of hearts at 3 dpi, one belonging to an unknown transgenic line (a and c), the other belonging to *Tg(Fli1a:EGFP)* (e-f). Yellow Arrows point to yellow contour done in Fiji for area measuring (a-d). BA stands for bulbus artriosus and V for ventricle. Scale bar: 100 μm.

The example heart observed with BF microscope has an infarct area that occupies approximately 12% of total ventricular area, while the example heart observed with LSFM microscope has an infarction size of 23% of total ventricular area (Fig. 9).

- **Bright-field (BF) Microscopy Limitations**

Though it is very useful, BF microscopy has a very important drawback that can harm sample visualization, which is sample thickness.

The cut shown in figure 9 has a thickness of 10 µm, whereas cuts represented in Fig. 10 are 6 µm thick. It is very noticeable the loss of shape integrity this difference (10 µm to 6 µm) can make (Fig. 10).

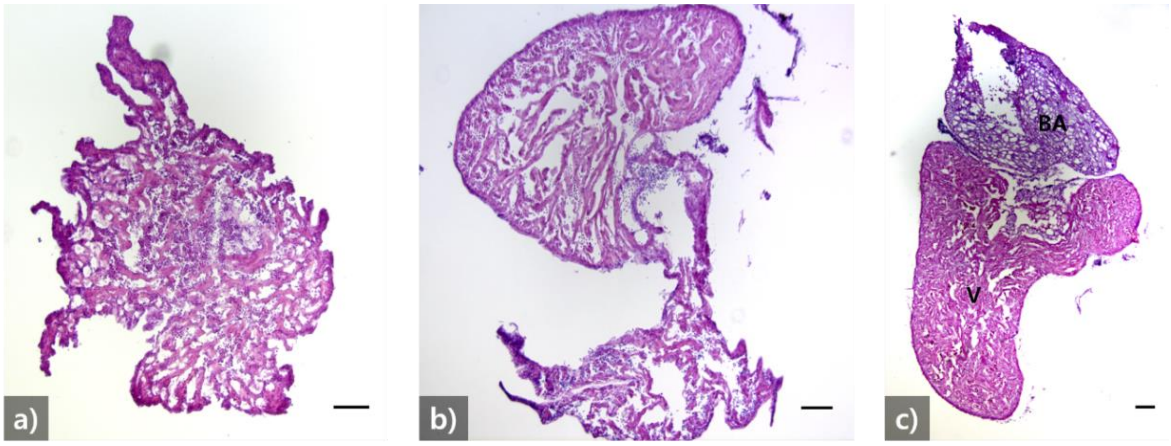

Fig. 10. Snapshots of histological cuts, with 6µm thickness, taken through BF microscope. Pictures of hearts belonging to an unknown transgenic line, at 1 dpi (c) and 3 dpi (a-b). BA stands for bulbus artriosus and V for ventricle. Scale bar: 100 µm.

- **Ligh Sheet Fluorescence Microscopy (LSFM) Limitations**

LSFM, as BF, also presents some limitations (including optical aberrations), but in this case, they are related to mounting medium quality.

Mounting solution needs to be being light permissive and without bubbles or small particles like dust, that can interfere with sample visualization. Here, mounting medium presented small bubbles, which interfered with sample's fluorescence by overshadowing (Fig. 11 – small white arrows).

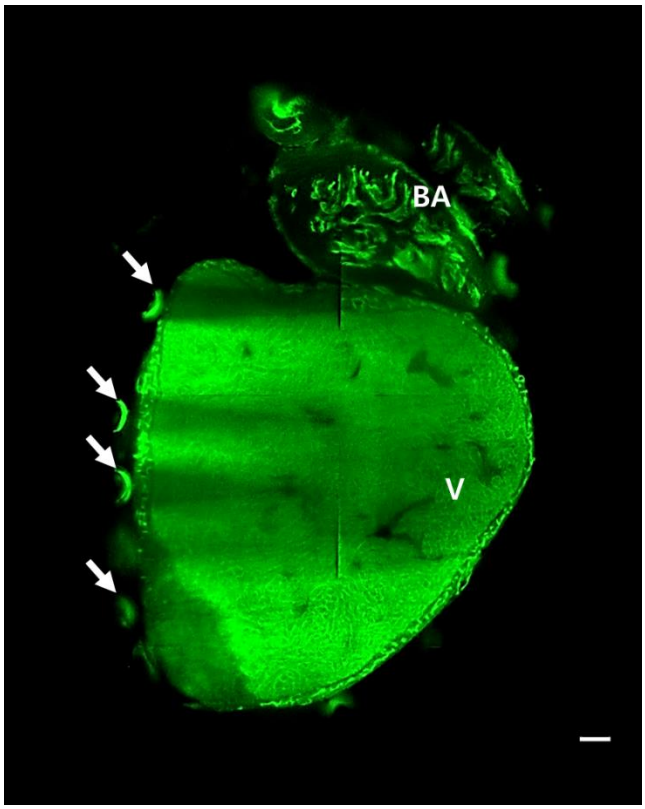

Fig. 11. Snapshot, taken in LSFM microscope, of cryocauterized heart showing mounting medium quality interference. Hearts belongs to *Tg(fli1a:EGFP)* transgenic line, at 1 dpi. Small white arrows point to artefacts (bubbles) present in mounting. BA stands for bulbus artriosus and V for ventricle. Scale bar: 100 μm.

Comparison of Different Transgenic Lines| Evaluation of Mortality, cryoinjury procedure control and Cardiac Tissue Histology

Nowadays there are numerous zebrafish transgenic lines that mark different cell types, and therefore different tissues or organs. As the project aimed to optimize all procedures of cryoinjury-induced MI in zebrafish adult fish, a comparison of several transgenic lines was performed regarding mortality, and heart repair at 1 dpi.

As aforementioned, the transgenic lines used were:

- *Tg(nestin-cre:GFP)*, that mark central and peripheral nervous system, as well as some kidney and heart cells (Kachinsky et al., 1995);
- *Tg(ras:EGFP)*, that mark cellular membrane (Chi et al., 2008);
- *Tg(kdrl:ras-cherry)*, that mark blood vessels' ECs (Cross et al., 2003);
- *Tg(cmlc2:GFP)*, that mark cardiomyocytes (Huang et al., 2003);

- *Tg(fli1a:EGFP)*, that mark ECs from both blood and lymphatic vessels, allowing imaging of vessel formation (Lawson and Weinstein, 2002).

- **Evaluation of Mortality**

From all transgenic lines used, *Tg(kdrl:ras-cherry)* presented the highest mortality percentage (50%) and *Tg(nestin-cre:GFP)* the lowest (6.3%). *Tg(fli1a:EGFP)*'s mortality percentage represents the normal regeneration model, that will be presented ahead (Fig. 12). It is important to refer that percentages displayed are merely demonstrative, as the number of fish used for each transgenic line was different.

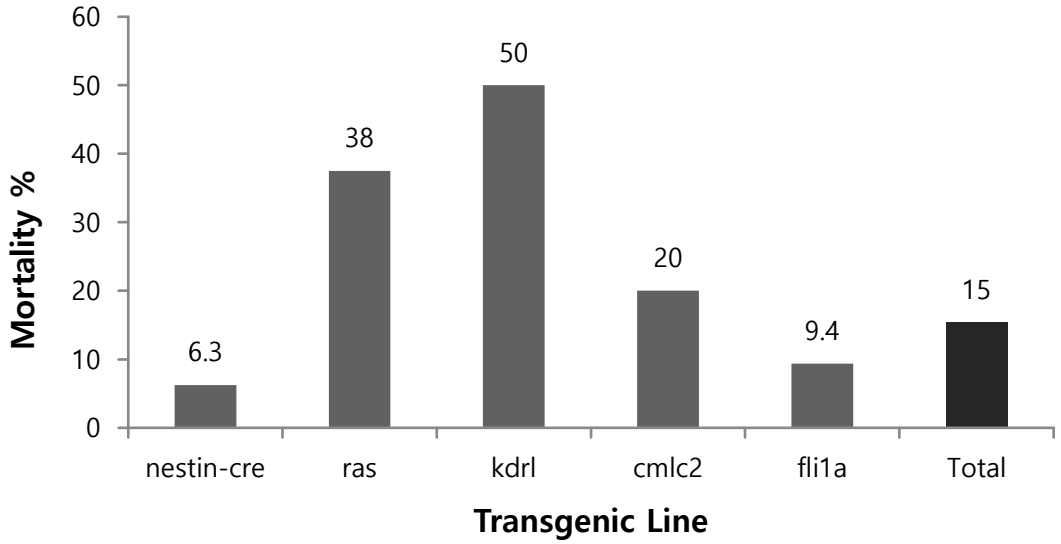

Fig. 12. Mortality percentage discriminated between transgenic lines. All transgenic lines used, are present in this graphic: *Tg(nestin-cre:GFP)*, *Tg(ras:EGFP)*, *Tg(kdrl:ras-cherry)*, *Tg(cmlc2:GFP)*, *Tg(fli1a:EGFP)*; along with total mortality percentage.

- **Evaluation of Cryoinjury Procedure Control**

Snapshots of procedure control through heart visualization 2 h after injury, show that there is an apparent difference between transgenic lines. Transgenic lines *Tg(nestin-cre:GFP)* and *Tg(cmlc2:GFP)* (Fig. 13a-b) both mark cardiomyocytes, presumably, and present a darker and more distinct infarcted area, since they have a higher, heart-localized, fluorescence when compared with other transgenic lines.

Tg(ras:EGFP)'s infarction is less apparent, since the fluorescence signal is much more generalized through whole-animal (Fig. 13c).

Tg(kdrl:ras-cherry) and *Tg(fli1a:EGFP)* are also very similar, with both having expression in ECs. Their aptitude to aid in vasculature observation is visible, especially in *Tg(fli1a:EGFP)*, as can be seen in the zoom cut-outs from Fig. 13d-e, where black arrowheads point to existing vessels.

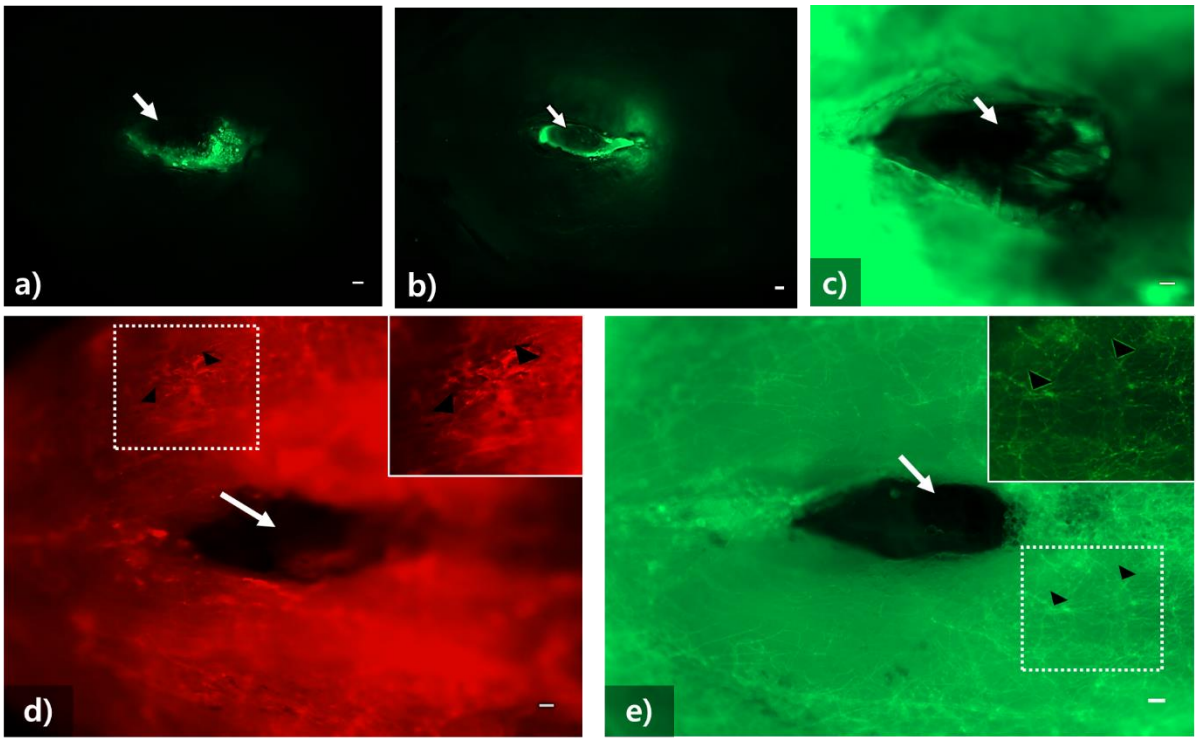

Fig. 13. Snapshots of injured hearts 2 hours' post-infarction, taken in Zeiss Axio Zoom V16 microscope. Fish belonging to *Tg(nestin-cre:GFP)* (a), *Tg(cmlc2:GFP) (b), Tg(ras:EGFP)* (c) and *Tg(fli1a:EGFP)* (e) present green fluorescence, and *Tg(kdrl:ras-cherry)* (d) presents red fluorescence signal. White arrows point to infarcted area (without fluorescent signal, and black arrowheads point to vessels. Scale bar: 100 μm.

- **Evaluation of Cardiac Tissue Histology**

This evaluation was done in terms of comparing different transgenic lines' cardiac tissue morphology to gather which provided the best imagining.

Generally, hearts belonging to *Tg(nestin-cre:GFP)* and *Tg(cmlc2:GFP)* transgenic lines have a greater difference in fluorescence between the ventricle and infarction areas than the remainder lines, since they mark heart muscle cells, cardiomyocytes (Fig. 14a-b).

With *Tg(ras:EGFP)* transgenic line the infarct area is visible, like with other lines, but it does not seem as evident, as fluorescence signal is alike between the infarct and ventricle (Fig. 14c).

Tg(kdrl:ras-cherry) line appears to be have a similar fluorescence signal to *Tg(fli1a:EGFP)* (snapshots of both regeneration models with blue contour), as they both mark ECs, with the infarcted area being much more fluorescent that the rest of the ventricle (Fig. 14d-f).

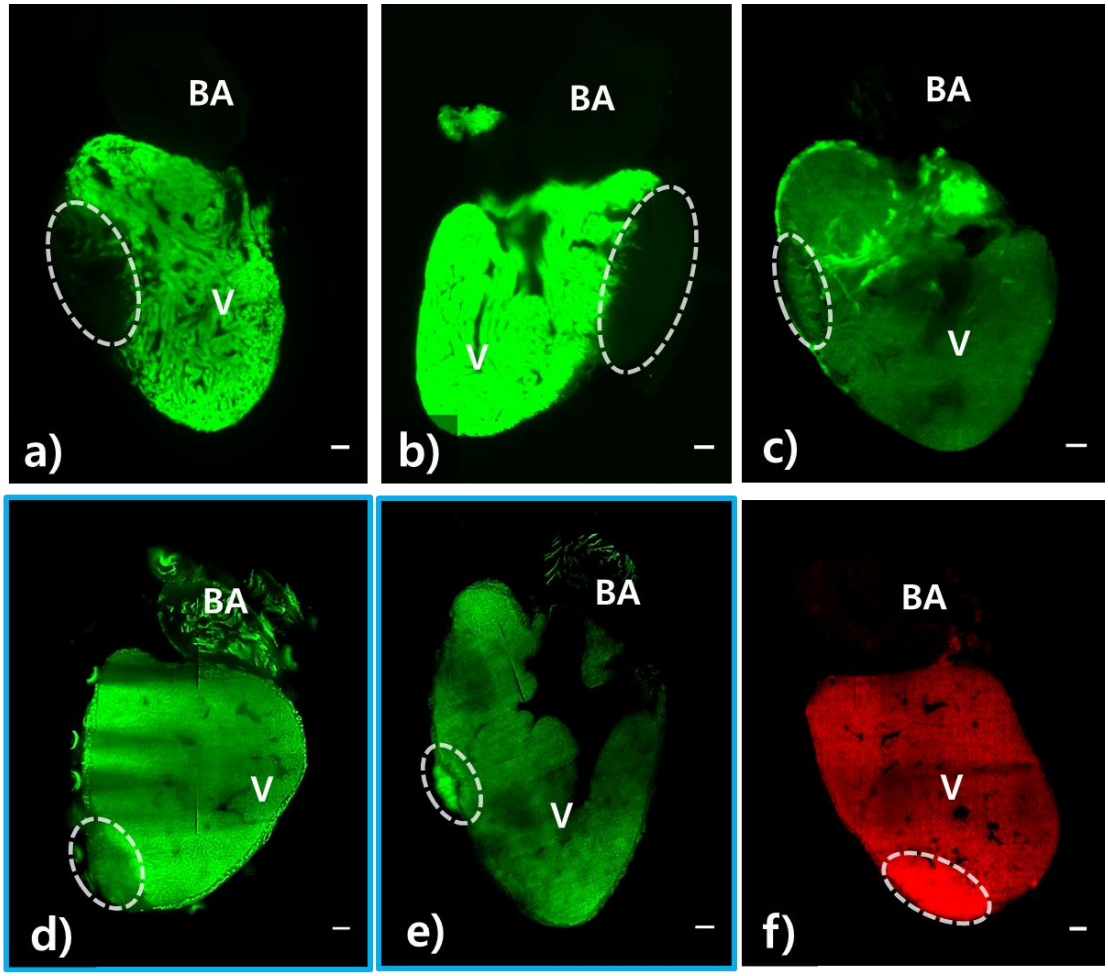

Fig. 14. Snapshots, taken in LSFM microscope, of cryocauterized hearts belonging to different transgenic lines at 1 dpi. *Tg(nestin-cre:GFP)* (a), *Tg(cmlc2:GFP)* (b), *Tg(ras:EGFP)* (c), and *Tg(fli1a:EGFP) (Normal Regeneration Model, d – Immunosuppression Model ,e)* present green fluorescence, and *Tg(kdrl:ras-cherry)* (f) presents red fluorescence signal. White oval dotted shapes represent the infarct in different areas of the ventricle (V). BA stands for bulbus artriosus. Scale bar: 100 μm.

COMPARISON OF NORMAL AND IMMUNOSUPPRESSION MODELS| EVALUATION OF MORTALITY, SCD40L AND CARDIAC TISSUE HISTOLOGY

As previous stated, the objective of this thesis was to establish protocols that will allow to continue the study of the evaluation of sCD40L in heart repair after cryoinjury-induced MI in adult fish, using *Tg(fli1a:EGFP)* transgenic line. To achieve that, a glucocorticoid-induced immunosuppression model will be used as a model of impaired repair after MI. In that perspective, the present thesis intent to compare the normal and immunosuppression models in terms of mortality, cardiac tissue histology and sCD40L concentrations.

- **Evaluation of Mortality**

It was observed that fish treated with beclomethasone possessed a higher mortality percentage (16%) than non-treated fish (9.4%).

The cumulative mortality percentage remained unchanged in the normal regeneration model since the 3 deaths occurred immediately after cryoinjury procedure (0 dpi). The immunosuppression model presents a critical point at 5 dpi, before which 5 fish died. After that time-point, only one fish died at 9 dpi (Fig. 15).

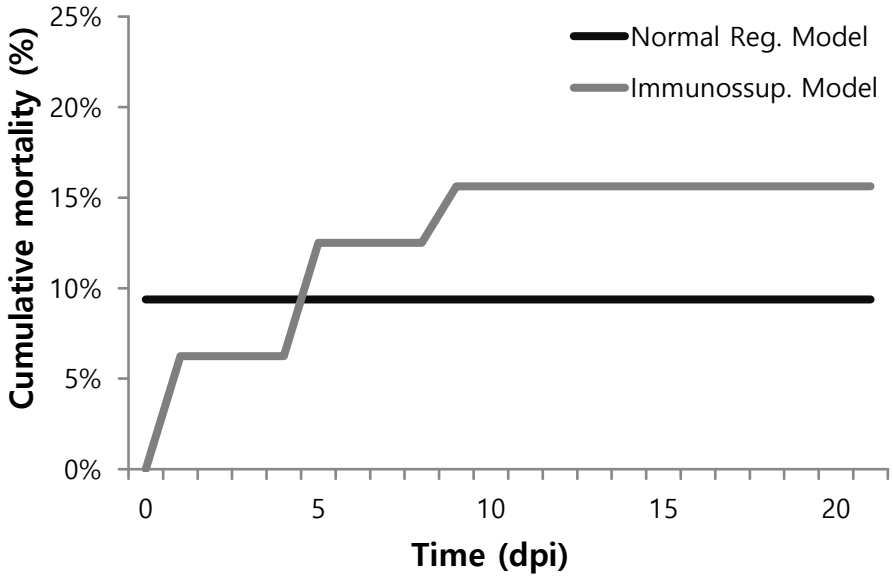

Fig. 15. Fish cumulative mortality percentage after cryoinjury induced-MI at different time-points.

- **Evaluation of sCD40L| Normal Model Longitudinal Variation and Dilution**

Results of ELISA assay show that sCD40L serum concentrations were higher for both models presented, when paralleled to control group (CTR), at all time-points (Fig. 16).

Considering the longitudinal variations of sCD40L in the normal regeneration model an increase of sCD40L level until 7 dpi was verified, followed by a decline to 21 dpi. However, the results must be interpreted with caution as much more fish should be analyzed.

In compromised regeneration model fish, sCD40L values were considerably higher than in fish of normal model. The longitudinal variation is also different, since a decrease until 21 dpi was verified.

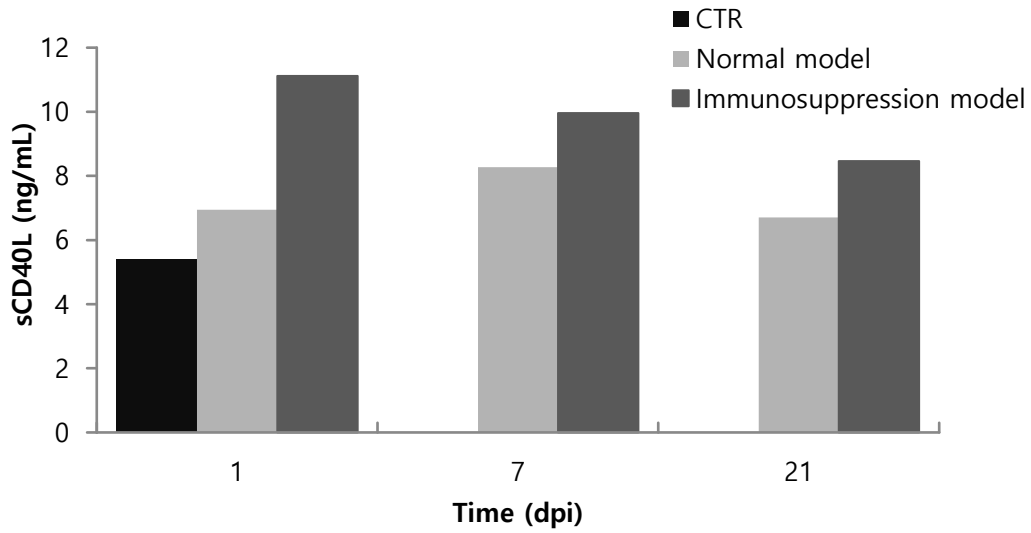

Fig. 16. Concentrations of sCD40L (ng/mL) after cryoinjury-induced MI in fish of normal regeneration and immunosuppression models at three different time-points (1 dpi, 7 dpi and 21 dpi).

Due to experimental constraints, data related to concentration of sCD40L at 3 dpi in both models was unsuitable to be individually compared as serum from other time-points. Even so, 3 dpi serum samples were able to be harnessed for ELISA and used in two ways: with (1:1) and without dilution. Concentrations of sCD40L were fairly similar in both cases (6.35 ng/ml and 7.35 ng/ml, correspondingly).

- **Evaluation of Cardiac Tissue Histology**

Further comparing both regeneration models, cardiac tissue morphology seems to be relatively different between them.

Immunocompromised fishes' infarct area emits much more fluorescence and has a fairly swollen aspect from 1 to 21 dpi (Fig. 17e-h). Unlike in normal model fish, which exhibit some signs of heart repair, like epicardium thickening, vessel formation and scar tissue (Fig. 17b-d), there does not seem to be visible repair among time-points, at least in the compromised regeneration model from this transgenic line.

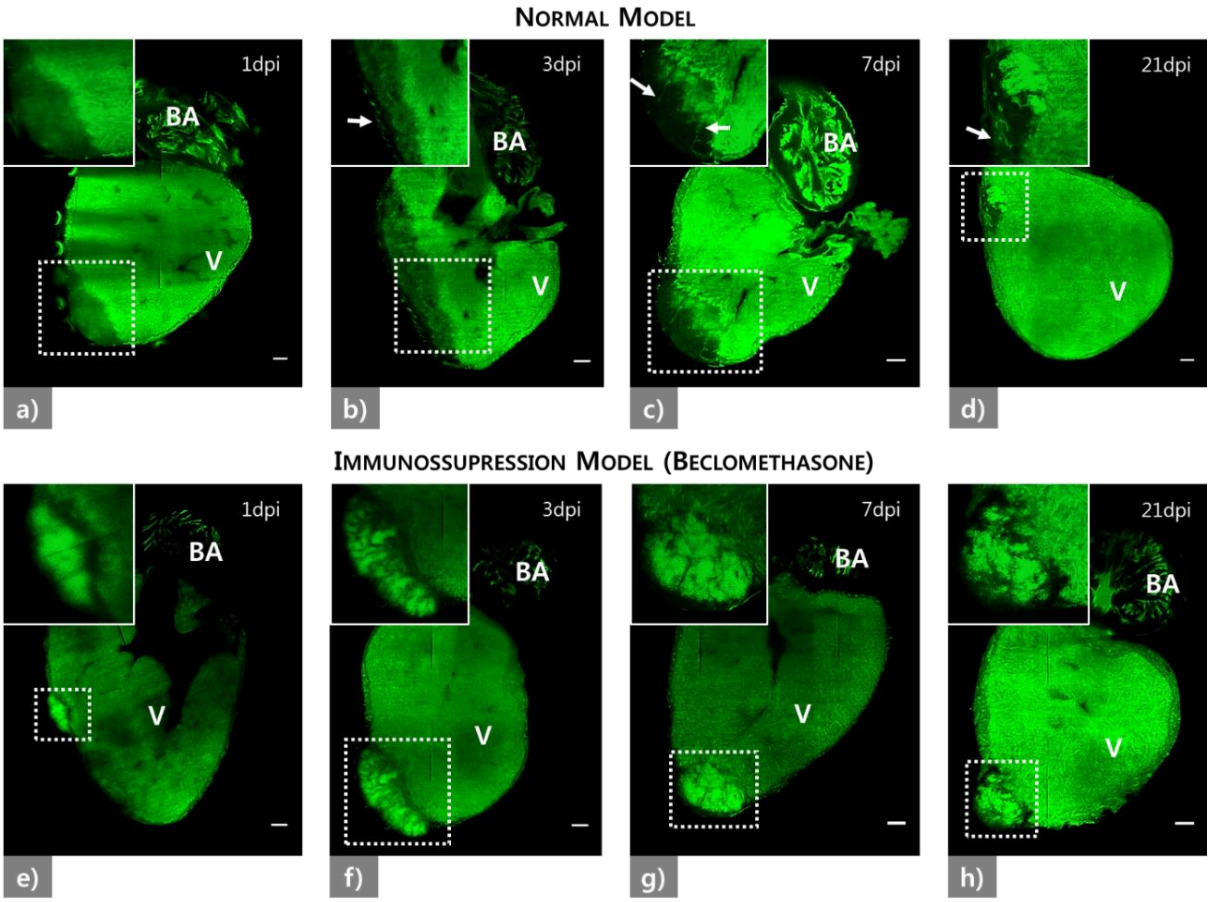

Fig. 17. Snapshots, taken in LSFM microscope, of cryocauterized hearts belonging to Normal Regeneration Model and Immunosuppression Model at 1, 3, 7 and 21 dpi. Small white arrows point to thickened epicardium (b), vessel formation (c) and scar-tissue (d). Dashed squares mark the infarcted area. BA stands for bulbus artriosus, and V for ventricle. Scale bar: 100 μm.

DISCUSSION

COMPARISON OF BLOOD COLLECTION METHODOLOGIES

Extracted blood's quantity and quality depends on several aspects: fish size, bigger fish, naturally, have more blood than smaller ones; researcher's technique dexterity, as with more practice, the easier and faster it is to collect larger volumes of blood; location/collection method, which is dependent on the previous point; collection time and time until centrifuging, longer times to gather blood and then to centrifuge (distance between collection and centrifugation sites should be considered), make it easier for hemolysis to occur (that said, the number of fish processed at any time-point should be around 2, but no more than 4); sudden movements, they should be avoided as to evade hemolysis; whether the procedure is terminal or not, which limits the methods that can be used, as well as the amount of blood that can be collected.

Blood collection from caudal area, by Zang et al., has proven to be an effective, rather easy method (with practice), as there is much less hemolysis and it is possible to obtain up to 8 µL of serum for analysis. It can be also much less invasive than other methods, such as tail cut and centrifugation with the fish alive and anesthetized (Babaei et al., 2013).

COMPARISON OF CLEARING PROTOCOLS

Through comparison of clearing protocols, it was observed that, unlike shown by Hama et al., Sca*l*eS does not render samples transparent better and faster than with Sca*l*eA2 (Hama et al., 2015). Quite the reverse, since Sca*l*eS did not, at all, clear zebrafish hearts and Sca*l*eA2 did.

Though Sca*l*eA2 did a good job clearing samples and preserved fluorescent signaling, it took about two plus weeks to do so, leaving the hearts frailer and with a

slightly visible higher volume, characteristics also discussed in other studies with different samples (Hou et al., 2015; Ke et al., 2013; Kuwajima et al., 2013).

Also, for this work, zebrafish hearts were placed into Sca*l*eA2 solution and left at 37ºC on orbital shaker, instead of RT as recommended on the original protocol (Hama et al., 2011). It was observed that the cleared much more easily, and faster, than at RT, where they took close to a month to be transparent.

COMPARISON OF MICROSCOPY METHODOLOGIES

Microscopy is a crucial tool to access heart repair, so a comparison of methodologies is always advantageous to assess which is best to apply for the sample used.

BF microscopy is more commonly used for histological studies than LSFM, which is more recent and allows 3D imaging. As literature using LSFM microscope for adult zebrafish heart and myocardial infarction imaging is scarce (Fei et al., 2016), this work serves a unique purpose.

In terms of sampling, for BF microscopy cut's thickness can seriously compromise overall sample structure integrity, which is crucial for a good visualization. With LSFM microscope, on the other hand, samples, if they are properly cared for, can be harnessed and used again, either to repeat an experiment or for further histological tests. This happens due to LSFM microscope being a less mechanically invasive method for the sample and the clearing process can be reversed (Hama et al., 2011).

LSFM allows 3D imaging, and therefore, trough rotation of the sample is possible to find the best angle and slice, in a way that it is not possible in BF microscopy, which depends on cryostat or paraffin cuts of the sample.

One important fact to bear in mind about LSFM, as shown in the results, is that it is very dependent on mounting solution quality, in terms of being light permissive and without bubbles or small particles like dust, that can interfere with sample visualization by

overshadowing it. Sample's transparency, is also crucial, in order to avoid light scattering, as the sheet of light needs to pass through the whole sample volume so that an image can be obtained without visual disruptions (Richardson and Lichtman, 2015).

Viewing-wise, in this dissertation, the 10 μm, thicker cuts in BF microscopy allowed a better viewing of infarct's morphological histology, as described in the results, its trabecular aspect, epicardium thickening and invasion of inflammatory cells (González-Rosa et al., 2011) due to hematoxylin and eosin staining that provided contrast between tissue structures. On LSFM that did not happen so effectively since the fluorescence was for a transgenic line-specific cell type, ECs. However, the protocol can be improved using other transgenic lines of zebrafish, such as *Tg(cmlc2:GFP)*; other immunofluorescence lesion staining like fibrinogen (to observe the fibrin layer that forms at 4dpi), tropomyosin (to observe cardiomyocytes), or proliferating cell nuclear antigen (for cell proliferation during regeneration); or double transgenics like *Tg(fli1a:EGFP, kdrl:ras-cherry)*, described in literature, in which blood vessels' ECs express both GFP and Cherry, but lymphatic vessels' ECs express only GFP, for example (Hogan et al., 2009).

Comparison of Different Transgenic Lines

Generally, transgenic fish from different lines (except *Tg(nestin-cre:GFP)* and *Tg(fli1a:EGFP)* from Normal Regeneration Model) have shown quite high mortality rates. These are older and frailer fish, with less resistance to both anesthesia and procedure.

In terms of cryoinjury procedure control through heart visualization 2 hours after procedure, transgenic lines are also very dissimilar. Transgenic lines *Tg(nestin-cre:GFP)* and *Tg(cmlc2:GFP)* are highly fluorescent since both mark cardiomyocytes and thus present a darker, more distinct infarcted area when compared with other transgenic lines, being the best ones to confirm infarct presence after procedure.

Zebrafish *Tg(nestin-cre:GFP)* is not a transgenic line commonly found in literature, specially associated with cardiovascular studies in adults, though *Tg(nestin-cre:GFP)* mice

are very used in neuroscience investigation (Dubois et al., 2006; Giusti et al., 2014; Sclafani et al., 2006).

Tg(cmlc2:GFP), a transgenic line with expression in differentiated cardiomyocytes under the cardiac myosin light chain 2 gene (*cmlc2*) promoter, has been used in studies of heart growth, cardiac function and morphogenesis studies (Chen et al., 2008; de Pater et al., 2009; Deacon et al., 2010).

Tg(kdrl:ras-cherry) and *Tg(fli1a:EGFP)* appear to have similar ventricular fluorescent histology, with different emission color (red and green, respectively). That can be explained by the fact they mark the same cell-type, ECs. Different infarct area histology, is most likely due to the first only targeting blood vessels' ECs, and Kdrl being a VEGF receptor (involved in angiogenesis), whereas the later targets both blood and lymphatic vessels' ECs (UniProt, 2016). Therefore, the *Tg(kdrl:ras-cherry)* line can be used to cross with other transgenic lines, like *Tg(fli1a:EGFP),* to complement specific tissue signal, as described above with *Tg(fli1a:EGFP, kdrl:ras-cherry)* (Hogan et al., 2009).

Tg(ras:EGFP) transgenic line, marking only cellular membrane, allows to see general cell presence in infarct area. *Ras* is not typically used on its own in a transgenic line, rather being placed under control of other promoters (since it helps to visualize cells' forms), like *kdrl* in *Tg(kdrl:ras-cherry)*, described above and in Han *et al.*; and *cmlc2*, used in other studies, as *Tg(cmlc2:ras-EGFP)* to mark individual cardiomyocytes with membrane-bound GFP (Chi et al., 2008; Han et al., 2016).

Comparison of Normal and Immunosuppression Models

A superior mortality percentage in immunosuppressed fish was to be expected, as their regeneration process has been compromised, making them more vulnerable to possible infection (though water was changed regularly). Interestingly, another observed side effect of exposure to beclomethasone, besides delay in heart repair and slightly

higher mortality, was extreme visible weight loss, though fish were fed every day. That fact difficult blood collection.

ELISA results, relative to concentrations of sCD40L, allowed to see a possible connection of its levels with cardiac repair, as fish from Immunosuppression Model appeared to have much higher concentrations of sCD40L in all time-points, that can perhaps support further studies that associate sCD40L with cardiac repair post-infarction and increase of cardiovascular events (Napoleão et al., 2015). However, there does not seem to be consensus on whether levels sCD40L might be related to cardiovascular disease due to it being necessary for event resolution, or due to it contributing to prolong disease; as, recently, lower levels of sCD40L have been associated with impaired repair after MI (Napoleão et al., 2016).

Through this work, it is feasible to conclude that it is possible to use samples of zebrafish blood with a dilution of 1:1 without much impairment on assessing sCD40L concentrations. This is very important as it allows to reduce the amount of blood needed for each pool, and as such, the number of fish used.

Histology-wise, there seems to be a rather apparent difference in infarct area morphology between models. Hearts from fish with compromised regeneration seem to have protuberance-like infarcts, from 1 dpi to 21 dpi. There appears to be a perturbation in the angiogenesis process, perhaps resulting in an induction of neovascularization in the infarcted area, that typically occurs around 14 dpi (Lien et al., 2012), which is a possible theory to explain the over-fluorescence seen in the immunosuppression model, in comparison with the normal model. There might be a chance of association with higher sCD40L concentration seen for the immunosuppression model (though further studies will be needed to confirm these preliminary levels), since sCD40L and CD40-CD40L system relation with VEGF has been suggested (Melter et al., 2000; Napoleão et al., 2016; Reinders et al., 2003). These observations would provide an interesting base subject for further investigations using *Tg(Fli1a:EGFP)*.

Unlike in normal model fish, which show signs of heart repair, epicardium thickening, vessel formation, and presence of scar tissue (González-Rosa et al., 2011). This gives the impression that glucocorticoids do interfere with regeneration post-myocardial infarction in zebrafish, as suggested by Huang et al (2013). However, it is difficult to make a straightforward comparison, since in this work, a cryoinjury model was used, instead of a resection model, like in Huang et al (2013).

CONCLUSIONS AND FUTURE PERSPECTIVES

Myocardial Infarction or necrosis of cardiac myocytes caused by prolonged ischemia, commonly known as a heart attack, is associated with an extremely high death-risk and other complications as humans are unable to significantly regenerate dead tissue. In contrast, adult zebrafish can regenerate ventricle's myocardium, endocardium and coronary vasculature entirely after cryoinjury. This process can be compromised by manipulation of its immune response with glucocorticoids.

Release of inflammatory mediators, such as CD40L, is an important part of healing process. CD40L is a transmembrane glycoprotein linked to cellular immunity and inflammation. So far, there is a possible correlation between its soluble form, sCD40L, and increased cardiovascular events in women, endothelial dysfunction and impaired myocardial repair post-MI.

The present dissertation allowed to establish several methodologies which will be important for future cardiovascular studies using zebrafish as animal model, such as cryoinjury, blood collection and heart histology. There has also been innovative work done in terms of using LSFM for cryoinjury observation, a state-of-the-art equipment for 3D imaging that allows a flawless, general morphological infarct evaluation.

Results have shown clear differences in infarction morphology between several transgenic lines available at iMM, and allowed to establish *Tg(cmlc2:GFP)* as the preferred transgenic line to be used in further studies involving evaluation of heart repair. These results were extremely useful to establish protocol procedures.

Comparison of zebrafish cardiac regeneration models seem to point out a difference, not only in terms of sCD40L levels in serum – which seems so match previous studies linking the glycoprotein to myocardial infarction – but also in aspect, as infarcts do look quite dissimilar, with infarcts in immunosuppressed fish being more protuberate and constant through time-points.

Conclusively, this thesis allowed implementing several methodologies necessary to further investigate the role of sCD40L on heart repair after cardiac injury in zebrafish. Therefore, this dissertation helped to lay down preliminary bases for future works to be done in this area.

REFERENCES

Alpert, J.S., Thygesen, K., Antman, E. and Bassand, J.P. (2000). Myocardial Infarction Redefined—A Consensus Document of The Joint European Society of Cardiology/American College of Cardiology Committee for the Redefinition of Myocardial Infarction. *J Am Coll Cardiol*. **36**, 959-969.

Aoyagi, Y., Kawakami, R., Osanai, H., Hibi,T., and Nemoto, T. (2015). A Rapid Optical Clearing Protocol Using 2,2′-Thiodiethanol for Microscopic Observation of Fixed Mouse Brain. *PLoS One*. **10**, e0116280.

Armitage, R.J., Fanslow, W.C., Strockbine, L., Sato, T.A., Clifford, K.N., Macduff, B.M., Anderson, D.M., Gimpel, S.D., Davis-Smith, T., Maliszewski, C.R., et al. (1992). Molecular and biological characterization of a murine ligand for CD40. *Nature*. **357**, 80-82.

Babaei, F., Ramalingam, R., Tavendale, A., Liang, Y., Yan, L.S., Ajuh, P., Cheng, S.H. and Lam, Y.W. (2013). Novel Blood Collection Method Allows Plasma Proteome Analysis from Single Zebrafish. *J Proteome Res*. **12**, 1580−1590.

Bakkers, J. (2011). Zebrafish as a model to study cardiac development and human cardiac disease. *Cardiovasc Res*. **91**, 279-288.

Betts, J.G., Desaix, P., Johnson, E., Johnson, J.E., Korol, O., Kruse, D., Poe, B., Wise, J.A., Womble, M., Young, K.A., et al. (2013). The Cardiovascular System: The Heart. In *Anatomy & Physiology*, pp. 777-836. OpenStax College.

Bonnefoy, J.Y. and Noelle, R.J. (1994). The CD40/CD40L interaction - all things to all immunologists. *Res. Immunol*. **145**, 199-249.

Carbone, E., Ruggiero, G., Terrazzano, G., Palomba, C., Manzo, C., Fontana, S., Spits, H., Kärre, K. and Zappacosta, S. (1997). A new mechanism of NK cell cytotoxicity activation: the CD40-CD40 ligand interaction. *J Environ Monit*. **185**, 2053-2060.

Chablais, F., Veit, J., Gregor, R. and Jaźwińska, A. (2011). The zebrafish heart regenerates after cryoinjuryinduced myocardial infarction. *BMC Dev Biol*. **11**, 21.

Chatzopoulou, A., Heijmans, J.P., Burgerhout, E., Oskam, N., Spaink, H.P., Meijer, A.H. and Schaaf, M.J. (2016). Glucocorticoid-Induced Attenuation of the Inflammatory Response in Zebrafish. *Endocrinology*. **157**, 2772-2784.

Chen, Z., Huang, W., Dahme, T., Rottbauer, W., Ackerman, M.J. and Xu, X. (2008). Depletion of zebrafish essential and regulatory myosin light chains reduces cardiac function through distinct mechanisms. *Cardiovasc Res*. **79**, 97-108.

Chen, C., Chai, H., Wang, X., Jiang, J., Jamaluddin, M.S., Liao, D., Zhang, Y., Wang, H., Bharadwaj, U., Zhang, S., et al. (2008). Soluble CD40 ligand induces endothelial dysfunction in human and porcine coronary artery endothelial cells. *Blood*. **112**, 3205-3216.

Chi, N.C., Shaw, R.M., De Val, S., Kang, G., Jan, L.Y., Black, L.B., and Stainier, D.Y.R. (2008). Foxn4 directly regulates tbx2b expression and atrioventricular canal formation. *Genes Dev*. **22**, 734-739.

Chiang, A.S., Lin, W.Y., Liu, H.P., Pszczolkowski, M.A., Fu, T.F., Chiu, S.F., and Holbrook, G.L. (2002). Insect NMDA receptors mediate juvenile hormone biosynthesis. *Proc Natl Acad Sci U S A*. **99**, 37-42.

Chung, K., Wallace, J., Kim, S.Y., Kalyanasundaram, S., Andalman, A.S., Davidson, T.J., Mirzabekov, J.J., Zalocusky, K.A., Mattis, J., Denisin, A.K., et al. (2013). Structural and molecular interrogation of intact biological systems. *Nature*. **497**, 332-337.

Cook, H.C. (1997). Origins of... Tinctorial methods in histology. *J Clin Pathol*. **50**, 716-720.

Costantini, I., Ghobril, J.P., Di Giovanna, A.P., Mascaro, A.L.A., Silvestri, L., Müllenbroich, M.C., Onofri, L., Conti, V., Vanzi, F., Sacconi, L., et al. (2015). A versatile clearing agent for multi-modal brain imaging. *Sci Rep*. **5**, 9808.

Cross, L.M., Cook, M.A., Lin, S., Chen, J.N. and Rubinstein, A.L. (2003). Rapid analysis of angiogenesis drugs in a live fluorescent zebrafish assay. *Arterioscler Thromb Vasc Biol*. **23**, 911-912.

de Pater, E., Clijsters, L., Marques, S.R., Lin, Y.F., Garavito-Aguilar, Z.V., Yelon, D. and Bakkers, J. (2009). Distinct phases of cardiomyocyte differentiation regulate growth of the zebrafish heart. *Development*. **136**, 1633-1641.

Deacon, D.C., Nevis, K.R., Cashman, T.J., Zhou, Y., Zhao, L., Washko, D., Guner-Ataman, B., Burns, C.G. and Burns, C.E. (2010). The miR-143-adducin3 pathway is essential for cardiac chamber morphogenesis. *Development*. **137**, 1887-1896.

Dodt, H.U., Leischner, U., Schierloh, A., Jährling, N., Mauch, C.P., Deininger, K., Deussing, J.M., Eder, M., Zieglgänsberger, W. and Becker, K. (2007). Ultramicroscopy: three-dimensional visualization of neuronal networks in the whole mouse brain. *Nat Methods*. **4**, 331-336.

Dubois, N.C., Hofmann, D., Kaloulis, K., Bishop, J.M. and Trumpp, A. (2006). Nestin-Cre transgenic mouse line Nes-Cre1 mediates highly efficient Cre/loxP mediated recombination in the nervous system, kidney, and somite-derived tissues. *Genesis*. **44**, 355-360.

Eames, S.C., Philipson, L.H., Prince, V.E. and Kinke, l. (2010). Blood Sugar Measurement in Zebrafish Reveals Dynamics of Glucose Homeostasis. *Zebrafish*. **7**, 205-213.

Ertl, G. and Frantz, S. (2005). Healing after myocardial infarction. *Cardiovasc Res*. **66**, 22-32.

Ertürk, A., Becker, K., Jährling, N., Mauch, C.P., Hojer, C.D., Egen, J.G., Hellal, F., Bradke, F., Sheng, M. and Dodt, H.U. (2012). Three-dimensional imaging of solvent-cleared organs using 3DISCO. *Nat Protoc*. **7**, 1983-1995.

Fei, P., Lee, J., Packard, R.R.S., Sereti, K.I., Xu, H., Ma, J., Ding, Y., Kang, H., Chen, H., Sung, K., et al. (2016). Cardiac light-sheet fluorescent microscopy for multi-scale and rapid imaging of architecture and function. *Sci Rep*. **6**, 22489.

Flood, P.M., Kelly, R., Gutiérrez-Heredia, L. and Reynaud, E.G. (2013). White paper: Sample Preparation for Light Sheet Microscopy. *Carl Zeiss Microscopy GmbH*. (Available Online).

Frangogiannis, N.G., Smith, C.W. and Entman, M.L. (2002). The inflammatory response in myocardial infarction. *Cardiovasc Res*. **53**, 31-47.

Frantz, S., Bauersachs, J. and Ertl, G. (2009). Post-infarct remodelling: contribution of wound healing and inflammation. *Cardiovasc Res*. **81**, 474-481.

Gauchat, J.F., Henchoz, S., Mazzei, G., Aubry, J.P., Brunner, T., Blasey, H., Life, P., Talabot, D., Flores-Romo, L., Thompson, J., et al. (1993). Induction of human IgE synthesis in B cells by mast cells and basophils. *Nature*. **365**, 340-343.

Giusti, S.A., Vercelli, C.A., Vogl, A.M., Kolarz, A.W., Pino, N.S., Deussing, J.M. and Refojo, D. (2014). Behavioral phenotyping of Nestin-Cre mice: implications for genetic mouse models of psychiatric disorders. *J Psychiatr Res*. **55**, 87-95.

González-Rosa, J.M., Martin, V., Peralta, M., Torres, M. and Mercader, N. (2011). Extensive scar formation and regression during heart regeneration after cryoinjury in zebrafish. *Development*. **138**, 1663-1674.

González-Rosa, J.M. and Mercader, N. (2012). Cryoinjury as a myocardial infarction model for the study of cardiac regeneration in the zebrafish. *Nat Protoc*. **7**, 782-788.

Graf, D., Muller, S., Korthauer, U., van Kooten, C., Weise, C. and Kroczek, R.A. (1995). A soluble form of TRAP (CD40 ligand) is rapidly released after T-cell activation. *Eur J Immunol*. **25**, 1749–1754.

Hama, H., Kurokawa, H., Kawano, H., Ando, R., Shimogori, T., Noda, H., Fukami, K., Sakaue-Sawano, A. and Miyawaki, A. (2011). Sca*l*e: a chemical approach for fluorescence imaging and reconstruction of transparent mouse brain. *Nat Neurosci*. **14**, 1481-1488.

Hama, H., Hioki, H., Namiki, K., Hoshida, T., Kurokawa, H., Ishidate, F., Kaneko, T., Akagi, T., Saito, T., Saido, T., et al. (2015). Sca*l*eS: an optical clearing palette for biological imaging. *Nat Neurosci*. **18**, 1518-1529.

Han, P., Bloomekatz, J., Ren, J., Zhang, R., Grinstein, J.D., Zhao, L., Burns, C.G., Burns, C.E., Anderson, R.M. and Chi, N.C. (2016). Coordinating cardiomyocyte interactions to direct ventricular chamber morphogenesis. *Nature*. **534**, 700-704.

Henn, V., Slupsky, J.R., Gräfe, M., Anagnostopoulos, I., Förster, R., Müller-Berghaus, G. and Kroczek, R.A. (1998). CD40 ligand on activated platelets triggers an inflammatory reaction of endothelial cells. *Nature*. **391**, 591-594.

Henn, V., Steinbach, S., Büchner, K., Presek, P. and Kroczek, R.A. (2001). The inflammatory action of CD40 ligand (CD154) expressed on activated human platelets is temporally limited by coexpressed CD40. *Blood*. **98**, 1047-1054.

Hogan, B.M., Herpers, R., Witte, M., Heloterä, H., Alitalo, K., Duckers, H.J. and Schulte-Merker, S. (2009). Vegfc/Flt4 signalling is suppressed by Dll4 in developing zebrafish intersegmental arteries. *Development*. **136**, 4001-4009.

Hou, B., Zhang, D., Zhao, S., Wei, M., Yang, Z., Wang, S., Wang, J., Zhang, X., Liu, B., Fan, L., et al. (2015). Scalable and DiI-compatible optical clearance of the mammalian brain. *Front Neuroanat*. **9**, 1-11.

Hristov, M., Gümbel, D., Lutgens, E., Zernecke, A. and Weber, C. (2010). Soluble CD40 ligand impairs the function of peripheral blood angiogenic outgrowth cells and increases neointimal formation after arterial injury. *Circulation*. **121**, 315-324.

Huang, C.J., Tu, C.T., Hsiao, C.D., Hsieh, F.J. and Tsai, H.J. (2003). Germ-line transmission of a myocardium-specific GFP transgene reveals critical regulatory elements in the cardiac myosin light chain 2 promoter of zebrafish. *Dev Dyn*. **228**, 30-40.

Huang, W.C., Yang, C.C., Chen, I.H., Liu, Y.M., Chang, S.J. and Chuang, Y.J. (2013). Treatment of Glucocorticoids Inhibited Early Immune Responses and Impaired Cardiac Repair in Adult Zebrafish. *PLoS One*. **8**, e66613.

Huisken, J., Swoger, J., Del Bene, F., Wittbrodt, J. and Stelzer, E.H.K. (2004). Optical Sectioning Deep Inside Live Embryos by Selective Plane Illumination Microscopy. *Science*. **305**, 1007.

Jagadeeswaran, P. and Sheehan, J.P. (1999). Analysis of Blood Coagulation in the Zebrafish. *Blood Cells Mol Dis*. **25**, 239-249.

Jopling, C., Sleep, E., Raya, M., Martí, M., Raya, A. and Belmonte, J.C.I. (2010). Zebrafish heart regeneration occurs by cardiomyocyte dedifferentiation and proliferation. *Nature*. **464**, 606-609.

Kachinsky, A.M., Dominov, J.A. and Miller, J.B. (1995). Intermediate filaments in cardiac myogenesis: nestin in the developing mouse heart. *J Histochem Cytochem*. **43**, 843-847.

Karpusas, M., Hsu, YM., Wang, J.H., Thompson, J., Lederman, S., Chess, L. and Thomas, D. (1995). A crystal structure of an extracellular fragment of human CD40 ligand. *Structure*. **3**, 1426.

Ke, M.T., Fujimoto, S. and Imai, T. (2013). SeeDB: a simple and morphology-preserving optical clearing agent for neuronal circuit reconstruction. *Nat Neurosci*. **16**, 1154-1161.

Ke, M.T., Nakai, Y., Fujimoto, S., Takayama, R., Yoshida, S., Kitajima, T.S., Sato, M. and Imai, T. (2016). Super-Resolution Mapping of Neuronal Circuitry With an Index-Optimized Clearing Agent. *Cell Rep*. **14**, 2718-2732.

Kikuchi, K., Holdway, J.E., Major, R.J., Blum, N., Dahn, R.D., Begemann, G. and Poss, K.D. (2011). Retinoic acid production by endocardium and epicardium is an injury response essential for zebrafish heart regeneration. *Dev Cell*. **20**, 397-404.

Kuwajima, T., Sitko, A.A., Bhansali, P., Jurgens, C., Guido, W. and Mason, C. (2013). Clear^{T}: a detergent- and solvent-free clearing method for neuronal and non-neuronal tissue. *Development*. **140**, 1364-1368.

Laman, J.D., de Smet, B.J.G.L., Shoneveld, A. and van Meurs, M. (1997). CD40-CD40L interactions in atherosclerosis. *Immunol Today*. **18**, 272-277.

Lawson, N.D. and Weinstein, B.M. (2002). In vivo imaging of embryonic vascular development using transgenic zebrafish. *Dev Biol*. **248**, 307-318.

Lederman, S., Yellin, M.J., Krichevsky, A., Belko, J., Lee, J.J. and Chess, L. (1992). Identification of a novel surface protein on activated CD4+ T cells that induces contact-dependent B cell differentiation (help). *J Exp Med*. **175**, 1091-1101.

Lien, C.L., Harrison, M.R., Tuan, T.L. and Starnes, V.A. (2012). Heart repair and regeneration: recent insights from zebrafish studies. *Wound Repair Regen*. **20**, 638-646.

Lin, H.H., Lai, J.S.Y., Chin, A.L., Chen, Y.C., and Chiang, A.S. (2007). A Map of Olfactory Representation in the Drosophila Mushroom Body. *Cell*. **128**, 1205-1217.

Mach, F., Schönbeck, U., Sukhova, G.K., Bourcier, T., Bonnefoy, J.Y., Pober, J.S. and Libby, P. (1997). Functional CD40 ligand is expressed on human vascular endothelial cells, smooth muscle cells, and macrophages: implications for CD40-CD40 ligand signaling in atherosclerosis. *Proc Natl Acad Sci U S A*. **94**, 1931-1936.

Major, R.J. and Poss, K.D. (2007). Zebrafish heart regeneration as a model for cardiac tissue repair. *Drug Discov Today Dis Models*. **4**, 219-225.

Mazzei, G.J., Edgerton, M.D., Losberger, C., Lecoanet-Henchoz, S., Graber, P., Durandy, A., Gauchat, J.F., Bernard, A., Allet, B. and Bonnefoy, J.Y. (1995). Recombinant soluble trimeric CD40 ligand is biologically active. *J Biol Chem*. **270**, 7025-7028.

McKay, R.G., Pfeffer, M.A., Pasternak, R.C., Markis, J.E., Come, P.C., Nakao, S., Alderman, J.D., Ferguson, J.J., Safian, R.D. and Grossman, W. (1986). Left ventricular remodeling after myocardial infarction: a corollary to infarct expansion. *Circulation*. **74**, 693-702.

Melter, M., Reinders, M.E., Sho, M., Pal, S., Geehan, C., Denton, M.D., Mukhopadhyay, D. and Briscoe, D.M. (2000). Ligation of CD40 induces the expression of vascular endothelial growth factor by endothelial cells and monocytes and promotes angiogenesis in vivo. *Blood*. **96**, 3801–3808.

Mescher, A.L. (2013). Histology & Its Methods of Study. In *Junqueira's Basic Histology*. McGraw-Hill Education.

Napoleão, P., Monteiro, M.C., Cabral, L.B., Criado, M.B., Ramos, C., Selas, M., Viegas-Crespo, A.M., Saldanha, C., Carmo, M.M., Ferreira, R.C., et al. (2015). Changes of soluble CD40 ligand in the progression of acute myocardial infarction associate to endothelial nitric oxide synthase polymorphisms and vascular endothelial growth factor but not to platelet CD62P expression. *Translacional Research*. **166**, 650-659.

Napoleão, P., Cabral, L.B.P., Selas M., Freixo, C., Monteiro, M.C., Criado, M.B., Costa, M.C., Enguita, F.J., Viegas-Crespo, A.M., Saldanha, C., et al. (2016). Stratification of ST-elevation myocardial infarction patients based on soluble CD40L longitudinal changes. *Translacional Research*. **176**, 95-104.

Pedroso, G.L., Hammes, T.O., Escobar, T.D., Fracasso, L.B., Forgiarini, L.F. and da Silveira, T.R. (2012). Blood Collection for Biochemical Analysis in Adult Zebrafish. *J Vis Exp*. **26**, e3865.

Peckham, M. (2011). Introduction to histology. In *Histology at a Glance*, pp. 12-13. United Kingdom: Wiley-Blackwell, Ltd.

Poss, K.D., Keating, M.T. and, Nechiporuk, A. (2003). Tales of regeneration in zebrafish. *Dev Dyn*. **226**, 202-210.

Poss, K.D., Wilson, L.G. and Keating, MT. (2002). Heart regeneration in zebrafish. *Science*. **298**, 2188-2190.

Rasmussen, T.L., Raveendran, G., Zhang, J. and Garry, D.J. (2011). Getting to the heart of myocardial stem cells and cell therapy. *Circulation*. **123**, 1771-1779.

Reinders, M.E., Sho, M., Robertson, S.W., Geehan, C.S. and Briscoe, D.M. (2003). Proangiogenic function of CD40 ligand-CD40 interactions. *J Immunol*. **171**, 1534-1541.

Renier, N., Wu, Z., Simon, D.J., Yang, J., Ariel, P. and Tessier-Lavigne, M. (2014). iDISCO: a simple, rapid method to immunolabel large tissue samples for volume imaging. *Cell*. **159**, 896-910.

Richardson, D.S. and Lichtman, J.W. (2015). Clarifying Tissue Clearing. *Cell*. **162**, 246-257.

Santilli, F., Basili, S., Ferroni, P. and Davì, G. (2007). CD40-CD40L system and vascular disease. *Intern Emerg Med*. **2**, 256-268.

Schindelin, J., Arganda-Carreras, I., Frise, E. Kaynig, V., Longair, M., Pietzsch, T., Preibisch, S., Rueden, C., Saalfeld, S., Schmid, B., et al. (2012). Fiji: an open-source platform for biological-image analysis. *Nat Methods*. **9**, 676-682.

Schnabel, K., Wu, C.C., Kurth, T. and Weidinger, G. (2011). Regeneration of cryoinjury induced necrotic heart lesions in zebrafish is associated with epicardial activation and cardiomyocyte proliferation. *PLoS One*. **6**, e18503.

Schönbeck, U., Varo, N., Libby, P., Buring, J. and Ridker, P.M. (2001). Soluble CD40L and cardiovascular risk in women. *Circulation*. **104**, 2266-2268.

Sclafani, A.M., Skidmore, J.M., Ramaprakash, H., Trumpp, A., Gage, P.J. and Martin, D.M. (2006). Nestin-Cre mediated deletion of Pitx2 in the mouse. *Genesis*. **44**, 336-344.

Staudt, T., Lang, M.C., Medda, R., Engelhardt, J. and Hell, S.W. (2007). 2,2'-thiodiethanol: a new water soluble mounting medium for high resolution optical microscopy. *Microsc Res Tech*. **70**, 1-9.

Susaki, E.A., Tainaka, K., Perrin, D., Kishino, F., Tawara, T., Watanabe, T.M., Yokoyama, C., Onoe, H., Eguchi, M., Yamaguchi, S., et al. (2014). Whole-brain imaging with single-cell resolution using chemical cocktails and computational analysis. *Cell*. **157**, 726-739.

Tainaka, K., Kubota, S.I., Suyama, T.Q., Susaki, E.A., Perrin, D., Ukai-Tadenuma, M., Ukai, H. and Ueda, H.R. (2014). Whole-body imaging with single-cell resolution by tissue decolorization. *Cell*. **159**, 911-924.

Tsai, P.S., Kaufhold, J.P., Blinder, P., Friedman, B., Drew, P.J., Karten, H.J., Lyden, P.D. and Kleinfeld, D. (2009). Correlations of Neuronal and Microvascular Densities in Murine Cortex Revealed by Direct Counting and Colocalization of Nuclei and Vessels. *J Neurosci*. **29**, 14553-14570.

Urbich, C., Dernbach, E., Aicher, A., Zeiher, A.M. and Dimmeler, S. (2002). CD40 ligand inhibits endothelial cell migration by increasing production of endothelial reactive oxygen species. *Circulation*. **106**, 981-986.

van Kooten, C and Banchereau, J. (2000). CD40-CD40 ligand. *J Leukoc Biol*. **67,** 2–17.

Vliegenthart, A.D., Starkey Lewis, P., Tucker, C.S., Del Pozo, J., Rider, S., Antoine, D.J., Dubost, V., Westphal, M., Moulin, P., Bailey, M.A., et al. (2014). Retro-Orbital Blood Acquisition Facilitates Circulating microRNA Measurement in Zebrafish with Paracetamol Hepatotoxicity. *Zebrafish*. **11**, 219-226.

Willems, I.E., Havenith, M.G., De Mey, J.G. and Daemen, M.J. (1994). The alphasmooth muscle actin-positive cells in healing human myocardial scars. *Am J Pathol*. **145**, 868-875.

Yang, B., Treweek, J.B., Kulkarni, R.P., Deverman, B.E., Chen, C.K., Lubeck, E., Shah, S., Cai, L. and Gradinaru, V. (2014). Single-cell phenotyping within transparent intact tissue through whole-body clearing. *Cell*. **158**, 945-958.

Zang, L., Shimada, Y., Nishimura, Y., Tanaka, T. and Nishimura, N. (2015). Repeated Blood Collection for Blood Tests in Adult Zebrafish. *J Vis Exp*. **102**, e53272.

Zeiss. (2016). ZEISS Lightsheet Z.1: Light Sheet Fluorescence Microscopy for Multiview Imaging of Large Specimens. (Available Online)